BOREAS An international journal of Quaternary research

Impact of climate change on sedimentation processes in the eastern Gulf of Finland during the Middle to Late Holocene

DARIA V. RYABCHUK, ALEXANDER Y. SERGEEV, DIANA V. PRISHCHEPENKO, VLADIMIR A. ZHAMOIDA, DARIA V. ELKINA, ALEXEY L. PISKAREV, LEYLA D. BASHIROVA, EKATERINA P. PONOMARENKO, LEONID M. BUDANOV, ANDREY G. GRIGORIEV AND ANTON V. EVDOKIMENKO

BOREAS

Ryabchuk, D. V., Sergeev, A. Y., Prishchepenko, D. V., Zhamoida, V. A., Elkina, D. V., Piskarev, A. L., Bashirova, L. D., Ponomarenko, E. P., Budanov, L. M., Grigoriev, A. G. & Evdokimenko, A. V.: Impact of climate change on sedimentation processes in the eastern Gulf of Finland during the Middle to Late Holocene. *Boreas*. https://doi.org/10.1111/bor.12500. ISSN 0300-9483.

This paper presents the results of high-resolution sedimentological analyses of sediment cores from the eastern Gulf of Finland (Baltic Sea). Sampling sites in the periphery of sedimentary basins were selected on the basis of acoustic profiling analyses. The research allowed tracing of the transition from the freshwater Ancylus Lake to the Littorina Sea. A specific transitional layer of 'blue clays', indicating the first stage of brackish water inflow into the Gulf of Finland, was dated to 9.1 ka BP. The date of first appearance of Littorina silty clay sedimentation was as follows: from 8.0 ka BP near Gogland Island, from 7.0 ka BP near Moshchny Island and from 5.9 ka BP near the Berezovye Islands. Holocene cycles of hypoxia, associated with periods of warming, were identified and cycles of 'warming – transgression – anoxic conditions' and 'cooling – regression – oxygen-rich conditions' were revealed. During the first stage of Littorina transgression (8.0–7.0 ka BP), the near-bottom environment in the deepest sedimentary basin of the eastern Gulf of Finland was characterized by oxygen deficiency. In contrast, 7.0–6.0 ka BP was dominated by oxygen-rich conditions and active processes of bioturbation. Anoxic conditions occurred again from 6.0–4.8 ka BP (Holocene Climatic Optimum), resulting in the accumulation of undisturbed silty clays with subhorizontal lamination. The interval from 4.8–2.0 ka was then characterized by oxygen-rich near-bottom conditions favourable for benthic organisms. The grain-size distributions throughout the sediment cores from the easternmost sedimentary basins suggest a relative lowering of the sea level from 3.5–1.8 ka and a rise after 1.8 ka BP.

Daria V. Ryabchuk (Daria_Ryabchuk@mail.ru), Alexander Y. Sergeev, Diana V. Prishchepenko, Vladimir A. Zhamoida, Leonid M. Budanov, Andrey G. Grigoriev and Anton V. Evdokimenko, AP Karpinsky Russian Geological Research Institute (VSEGEI), 74, Sredny pr., St. Petersburg, 199106, Russia; Daria V. Elkina and Alexey L. Piskarev, Gramberg All-Russia Research Institute of Geology and Mineral Resources of the World Ocean, St. Petersburg, 199106, Russia and Institute of Earth Sciences, St. Petersburg State University, St. Petersburg 199134, Russia; Leyla D. Bashirova, Shirshov Institute of Oceanology, Russian Academy of Sciences, Nahimovskiy prospect, 36, Moscow, 117218, Russia and Immanuel Kant Baltic Federal University, A. Nevskogo str., 14, Kaliningrad, 236041, Russia; Ekaterina P. Ponomarenko, Shirshov Institute of Oceanology, Russian Academy of Sciences, Nahimovskiy prospect, 36, Moscow, 117218, Russia; *received 9th May 2020, accepted 5th November 2020.*

The Baltic Sea, with an area of 415 266 km^2 and a large catchment area of 1 641 400 km^2, is one of the largest relatively shallow (average depth of about 50 m) semi-enclosed brackish water seas. A large amount of sediment is delivered by the numerous rivers draining the catchment area of the Baltic Sea basin, which is separated from the North Sea and the Atlantic Ocean by a shallow area in its western part. These conditions contribute to the relatively high sedimentation rates experienced in the Baltic Sea (ranging from about 1–6 m ka^{-1}; Ignatius 1958; Mattila *et al.* 2006). Consequently, the Baltic Sea provides a high-resolution bottom sediment archive covering, from the geological perspective, a relatively short time period – from centuries to thousands of years. Therefore, the Baltic Sea sediments provide a good source for analyses of environmental and climate changes since the last deglaciation.

According to existing understanding, there have been several stages in the postglacial development of the Baltic Sea region: the glaciolacustrine Baltic Ice Lake (16.0–11.7 ka BP); the slightly brackish water Yoldia Sea (11.7–10.7 ka BP); the freshwater Ancylus Lake (10.7–9.8 ka BP); the Initial Littorina (or Mastogloia) Sea (9.8–8.5 ka BP); the Littorina Sea (8.5–4.5 ka BP); and the post-Littorina Sea (or the Baltic Sea) (since 4.5 ka BP) (Andrén *et al.* 2011).

It should be mentioned that in the eastern Gogland Basin, the short-lived Yoldia Phase was marked both by an initial phase (a 3-cm mud layer enriched with organic matter) and an end phase (with lower content of organic matter) (Harff *et al.* 2011). The history of the Yoldia Sea stage investigation within the coasts and offshore of the eastern Gulf of Finland (EGoF) has been described in detail by Spiridonov *et al.* (2007). According to latest studies (Raukas 1994), the EGoF corresponds with the easternmost part of the Yoldia Sea.

Several studies undertaken in different areas of the Baltic Sea (Sandgren *et al.* 2004; Miettinen *et al.* 2007; Harff *et al.* 2011, Harff *et al.* 2017; Virtasalo *et al.* 2011; Rosentau *et al.* 2013; Kotilainen *et al.* 2014; Ryabchuk *et al.* 2016; Warden *et al.* 2017) have enabled significant advances in knowledge about climate-related changes to palaeobasin sedimentation. The most comprehensive results from palaeorecontructions of the postglacial basin development are based on the study of 9–12 m long

DOI 10.1111/bor.12500

sediment cores from the Central Baltic (Grigoriev *et al.* 2011; Harff *et al.* 2011) containing complete postglacial sequences without hiatuses.

In Russia, geological investigations in the EGoF have been carried out, as part of the State geological mapping at a scale of 1:200 000, since the 1980s by the Department of Marine and Environmental Geology of the A.P. Karpinsky Russian Geological Research Institute (VSEGEI). By 2000, the gulf bottom had been investigated by a series of sub-bottom profiles (SBP) covering more than 6000 km and involving more than 6000 sampling sites (including 4000 gravity cores). This work resulted in the compilation of a set of geological maps showing pre-Quaternary and Quaternary deposits, as well as bottom sediments (Petrov 2010). These represent a unique archive of raw geological and geophysical data.

The first results of high-resolution sedimentological research in the EGoF have been obtained through the international project BONUS INFLOW (2007–2009) (Virtasalo *et al.* 2014). An applied multiproxy approach has proven to be highly efficient. For the first time, detailed data about the transition from the freshwater Ancylus Lake to the marine Littorina environment have been obtained, and evidence of the Neva River onset has been documented.

The transition sediment layer from freshwater to the marine environment was first described by Ignatius *et al.* (1968). The layer was specified to comprise 'blue clays' with thickness from 1 to 10 cm and was recovered in the EGoF during the State geological mapping process. The deposits have since been analysed in detail by Virtasalo *et al.* (2010). In the northern Baltic Sea, the thickness of such deposits is 46 cm (MGML and AS2 cores; Virtasalo *et al.* 2010). The deposits overlie the typical Ancylus silty clay enriched by amorphous iron-sulphides. It is possible to subdivide the deposits into two layers with a gradational contact: grey clays with patchy enrichment by dispersed organic matter (32 cm) and bluish-grey clays (14 cm). To date, only two cores taken in the EGoF (09BI-3 and 17G30-2) contained sequences with a 'blue clays' layer (6–8 cm thick). A high-resolution study of the cores has shown that bottom and top contacts of the layer are enriched with sand and silt fractions (Ryabchuk *et al.* 2017).

The present paper aims to reveal regional details of postglacial geological development of the EGoF in the context of climate change during the last 10 000 years, including characterization of the near-bottom hydrodynamics of postglacial basins. It also aims to establish the timing and environmental changes such as transgressions/regressions, and oxic/anoxic conditions in different sedimentary basins of the EGoF during the Holocene.

Study area

The Russian part of the Gulf of Finland includes the easternmost part of this narrow gulf located in the northeastern part of the Baltic Sea. The gulf is 420 km in length, with the Russian part being 140 km. Its width varies from 70 km at its narrow western entrance to 130 km at its widest part at the Moshchny Island meridian (Fig. 1). The total area of the Gulf of Finland is just under 30 000 km^2, the Russian part is a little over 11 000 km^2.

The main characteristics of the EGoF are: (i) low rates of recent (last 2000 years) glacio-isostatic rebound (0–2 mm a^{-1}) and slow relative sea-level rise (according to the data obtained from a Kronshtadt sea-gauge, the rate of sea-level rise from 1835 to 2005 was 0.7 mm a^{-1}) (Gordeeva & Malinin 2014); (ii) relative shallowness, with the average water depth being 20 m and a maximum of 92 m to the west of Gogland Island (Petrov 2010); (iii) relatively low relief contrast caused by accumulation and erosion processes; and (iv) Holocene mud accumulation localized within sedimentary basins positioned at water depths ranging from 5 m in Neva Bay, to 70–80 m in the vicinity of Gogland Island (Ryabchuk *et al.* 2018).

The easternmost part of the Gulf of Finland is mostly covered by Quaternary deposits with a thickness of 30 m on average (Petrov 2010). Maximal (100–120 m) thickness of Quaternary deposits has been observed within palaeovalleys; these are typical features of the bedrock surface in the southern and eastern parts of the study area, where crystalline and metamorphic rocks of the Baltic Shield are covered by Vendian sandstones, siltstones, clays, and mixed sediments (Petrov 2010).

There are several sources of clastic sediment input to the EGoF. The total average annual river sediment load is relatively small, at 800–1100 thousand tonnes contributed by the Neva River (510–556 kT); the Narva River (136–160 kT); Kymijoki River (50 kT), the Luga River at 40.8 kT, and other rivers contributing a further 51.3 kT (Gudelis & Emelyanov 1976; Nezhikhovsky 1998; Rasmus *et al.* 2015; Sokolov 2016). A 3-year study of currents and turbidity flows in two locations of the EGoF, at depths of 41 and 44 m, showed that the average annual sediment resuspension was approximately 5–20 kg m^{-2} (Rasmus *et al.* 2015). Based on the data obtained, at least 40 million tons of sediment are redistributed annually within the EGoF due to erosion processes. Due to the existence of extensive shallow nearshore areas and significant depth of wave impact during extreme storms and surges (approximately 5 m) (Ryabchuk *et al.* 2011), coastal erosion, transportation, and redeposition provide another source of material.

The EGoF acoustic stratigraphy of Quaternary deposits has generally been well known since the 1980s (Spiridonov *et al.* 1988, 2007; Winterhalter 1992) and has been supported by geological and geophysical research undertaken since that time (Kaskela *et al.* 2017; Budanov *et al.* 2019; Ryabchuk *et al.* 2020a). It has been shown that acoustic units (AUs) distinguished on the SBP correspond to the different Baltic Sea evolution stages (Ryabchuk *et al.* 2020a). Geological interpretation of SBP is supported by the results collected from more

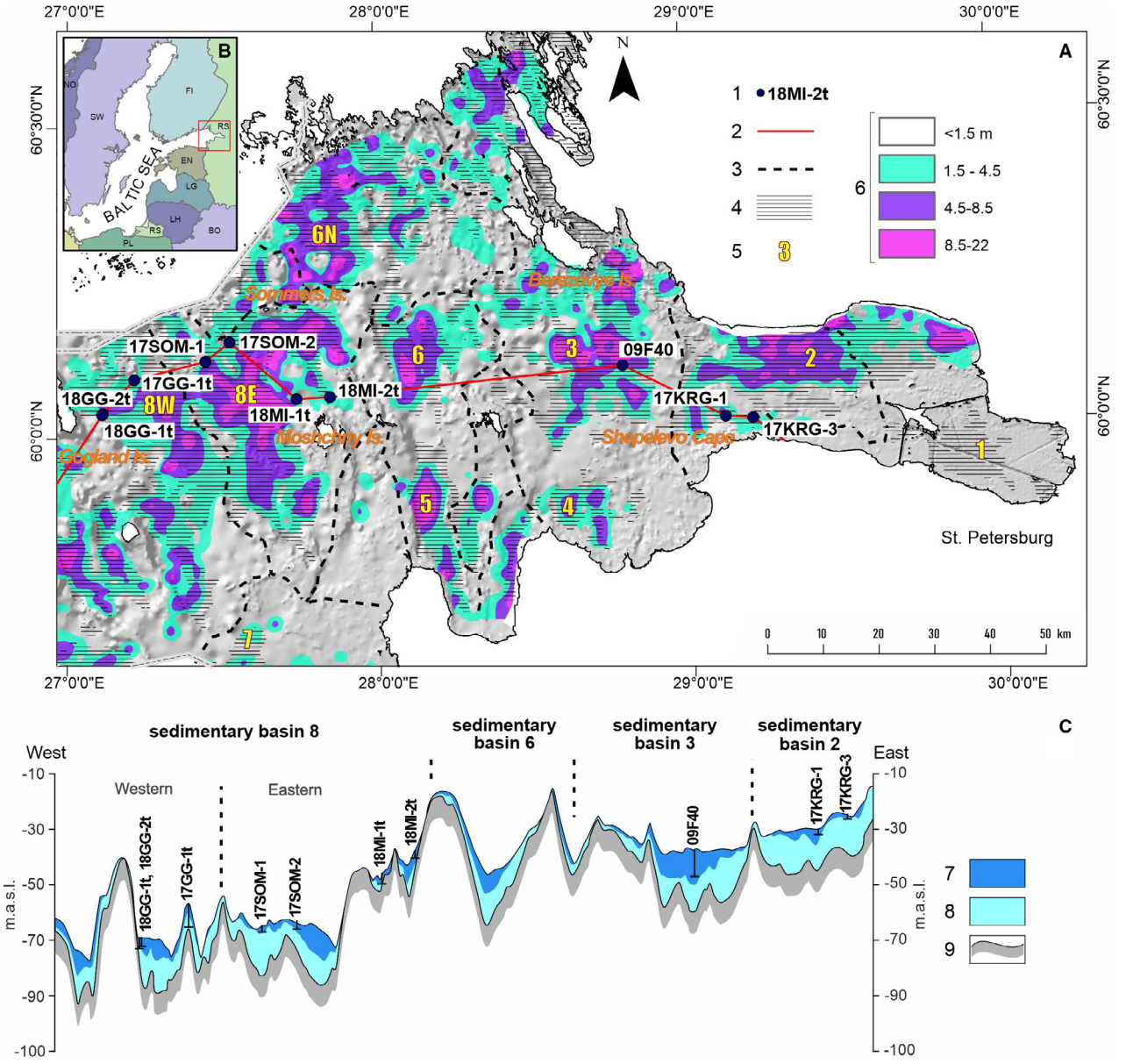

Fig. 1. A. Location of the sediment cores in the study area on the scheme of the Holocene sediment thickness. 1 = sediment sampling sites; 2 = location of the geological profile; 3 = boundaries of sedimentary basins; 4 = areas of modern silty clay accumulation; 5 = indexes of sedimentary basins; 6 = thickness of the Holocene deposits according to SBP (m). B. Study area shown on a map of the Baltic Sea region. C. Geological profile (for location, see the red line in panel A): 7 = Holocene deposits; 8 = Pleistocene glaciolacustrine deposits (the Baltic Ice Lake homogenous and varved clays); 9 = Last Glacial till surface (acoustic fundament).

than 4000 long sediment cores (metadata are available at https://www.emodnet-geology.eu/map-viewer/?p=boreholes).

It is noteworthy that due to an occurrence of distinct acoustic boundaries and unconformities (Budanov *et al.* 2019), boundaries such as till surface and Late Pleistocene clays surface can successfully be traced based on acoustic profiles. This allows interpolation of the boundaries verified by sediment sampling for the whole area of the EGoF bottom.

According to the lithological description of the cores, sediments of different stratigraphical units are characterized by very distinct lithological features, differing in colour, density and sediment structure (Spiridonov *et al.* 1988, 2007). The classification of the lithostratigraphical units in the sediments of the Baltic Sea has been developed based on this approach; the lithostratigraphical units have furthermore been attributed to the main phases of the postglacial basin development of the Baltic Sea (Spiridonov *et al.* 2007).

Material and methods

For the present study, sediment cores from the EGoF were taken during the 35th cruise of the R/V 'Academic Nikolaj Strakhov' (21st–24th July 2017) and several cruises of the R/V 'SN-1303' (9th–11th September 2017 and 23rd–28th July 2018) using a gravity corer (Fig. 1, Table 1). Sampling sites were chosen based on archives of SBP data obtained during State geological mapping (1985–2000) (digitized and transformed into *.sgy format) and numerous projects undertaken in the period 2004–2018. The peripheral parts of sedimentary basins were chosen to obtain shorter sediment sequences (with erosion layers and sediment hiatuses) covering the same time-span as the thicker successions in the central part of the basins (Fig. 1). To obtain the acoustic data, continuous acoustic profiling using an EdgeTech 3300-HM sub-bottom profiler (pinger type system) with Discover Sub-Bottom v3.36 software (R/V 'Academic Nikolaj Strakhov') and GEONT-HRP 'Spektr-Geophysika' Ltd. sub-bottom profiler (boomer and sparker type system) (R/V 'SN-1303') was used.

There are differences between the three above mentioned types of sources: they produce signals of various energy and frequency and therefore perform different penetration and instrumental resolution. Pinger generates the highest frequency signal (2–16 kHz) and provides penetration below the bottom up to 30 m with vertical resolution 3–20 cm. Boomer has a lower frequency signal (1–2.5 kHz) with penetration up to 100 m and vertical resolution 15–40 cm. Sparker produces the lowest frequency signal (0.2–1 kHz) and provides penetration up to 300 m with vertical resolution 0.3–2 m.

The AUs were assigned based on the approaches described in detail in Ryabchuk *et al*. (2020b) and Spiridonov *et al*. (2007). To investigate the modern sedimentary conditions within the sampling sites, surface sediments were taken using a box-corer.

Special attention was paid both to acquiring the sediment sections capturing the transition from the freshwater Ancylus Lake to the marine Littorina Sea environment and to showing the hiatuses within the sections. Nine cores from 105 to 482 cm long were chosen for the high-resolution sedimentological study (Fig. 2, Table 1). Onboard, the cores were packed in plastic pipes 1 m in length, and they were sealed and stored in cool conditions (4 °C) during transportation to the laboratory. Once in the VSEGEI laboratory, the cores were split into two sections for lithological description using the Munsell Soil Colour Charts combined with digital photography. The stratigraphical units were assigned on the basis of lithological description of the studied sediment cores (Spiridonov *et al*. 2007). The units were compared with reinterpreted archive data to improve the map of the Quaternary deposits by assigning the low-thickness 'blue clays' layers to the transition phase between the freshwater Ancylus Lake and Littorina Sea.

Additionally, the 09F40 sediment core (509 cm long) taken in the sedimentary basin south of Berezovye Islands during the joint scientific cruise of the VSEGEI and the Geological Survey of Finland onboard Finnish R/V 'Aranda' (2009), was used in the study for comparison. The upper 500 cm of the core represents Littorina and post-Littorina deposits (last 5.8 ka), with an erosional surface between the sediments at 200 cm dated to 3.4 ka BP (Fig. 1, Table 1). The discontinuity at 500 cm indicates the upper boundary of the Ancylus Lake (Virtasalo *et al.* 2014).

Studied cores were analysed for the distribution of grain size (sampled every 1 cm, with a total of 1858 samples) using the laser diffraction particle size analyser 'Microsizer 201A' (VA Instal, Russia). The device permits the measurement of grain size (particle diameter) in the 1 to 300 μm range. An ultrasonic bath with sodium tripolyphosphate solution was used for dispersion of the particles before the measurement. An X-ray fluorescence spectrometer (Innov-X, OLYMPUS) was applied for the detection of Al, Si, P, S, Cl, K, Ca, Ti, V, Cr, Mn, Fe, As, Y, Zr, Ba and Pb. Measurements were undertaken along the core sections (every 2 cm). For this purpose, a measuring

Table 1. Location of sediment cores from the EGoF.

Core name	Research vessel, date	Latitude N (WGS 84)	Longitude E (WGS 84)	Water depth (m)	Core length (cm)
09F40	R/V 'Aranda', 6.08.2009				
(MGML-2009-4		60°06.408	28°47.521	38.0	509.0
MGML-2009-5)		60°06.409	28°47.518	38.0	454.0
17GG-1t	R/V 'Academic Nikolaj Strakhov', 35th cruise, 22.07.2017	60°05.698	27°12.899	58.0	482.0
17SOM-1	R/V 'SN-1303', 13.09.2017	60°07.431	27°26.705	62.0	142.0
17SOM-2	R/V 'SN-1303', 13.09.2017	60°08.480	27°43.398	55.0	152.0
17KRG-1	R/V 'SN-1303', 14.09.2017	60°01.268	29°07.163	30.0	114.0
17KRG-3	R/V 'SN-1303', 14.09.2017	60°01.046	29°12.460	27.0	105.0
18GG-1t	R/V 'SN-1303', 26.06.2018	60°02.306	27°06.757	65.0	198.0
18GG-2t	R/V 'SN-1303', 26.06.2018	60°02.389	27°06.865	67.0	267.0
18MI-1t	R/V 'SN-1303', 28.06.2018	60°03.747	27°44.293	50.0	216.0
18MI-2t	R/V 'SN-1303', 28.06.2018	60°03.890	27°50.831	43.0	177.0

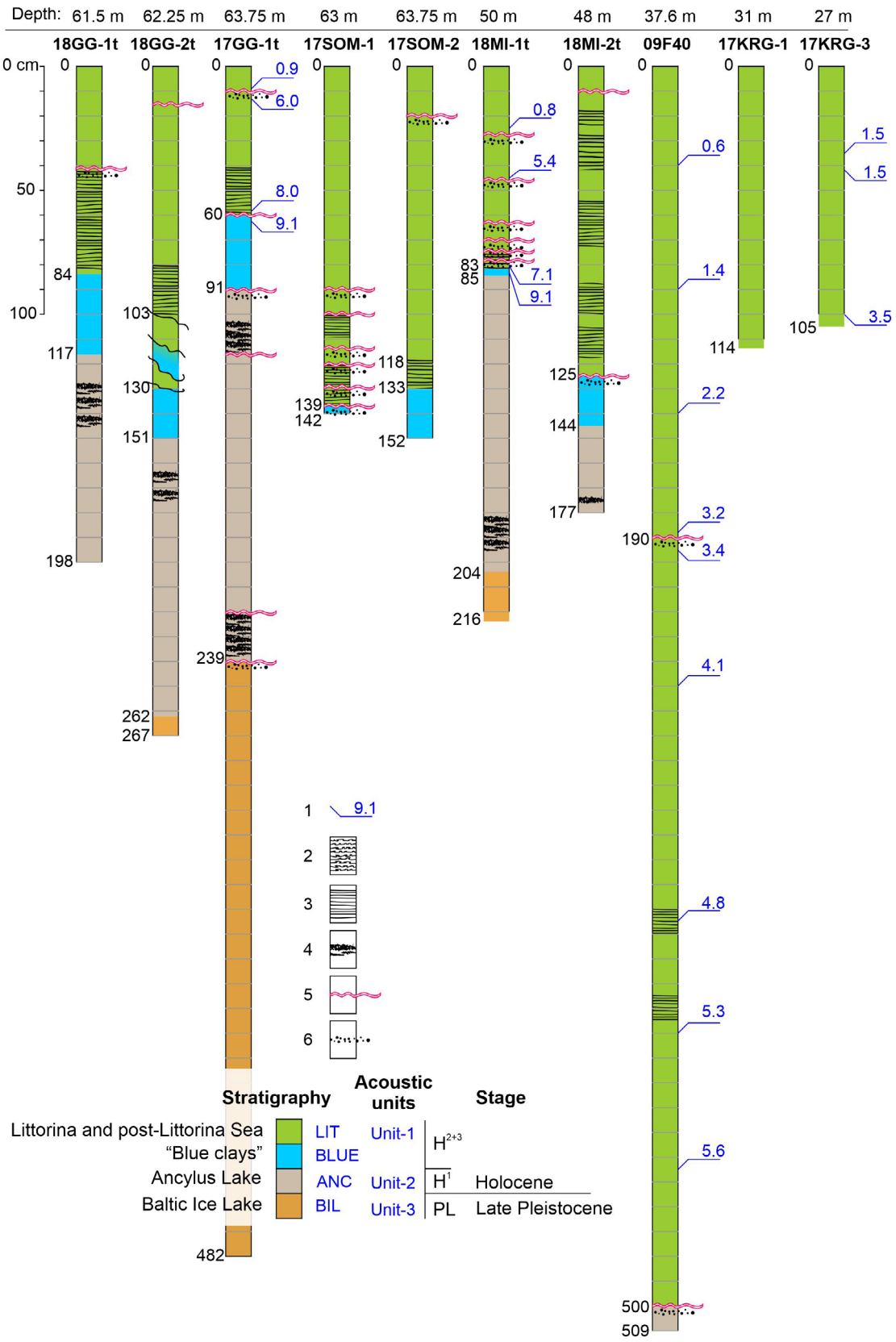

Fig. 2. Lithology of studied sediment cores from the EGoF. 1 = Results of AMS radiocarbon dating (ka BP); 2 = partly laminated bioturbated sediments; 3 = laminated sediments; 4 = hydrotroillite (amorphous Fe-sulphides) layers; 5 = erosion surfaces; 6 = enrichment with sand material.

window with a tubular analyser was installed on the core surface, the latter being covered with a 17-μm-thick plastic film to prevent disturbance of the core surface. The exposure time for each measurement was 60 s.

Additionally, six cores (17GG-1t, 17KRG-1, 17SOM-1, 17SOM-2, 18GG-2t and 18MI-1t) were studied (every 3 cm, using 1-cm-thick slices) using an X-ray scanning crystal-diffraction spectrometer 'SPEKTROSKAN-MAKS-G' to measure the concentration of Sr, Pb, As, Zn, Cu, Ni, Co, Fe_2O_3, TiO_2, MnO, V, Cr and Br. Prior to analysis, the samples were dried at 20 °C and ground. Distribution of Br concentration throughout the sediment section was used as a palaeosalinity proxy (Grigoriev *et al.* 2011). This method was first developed at VSEGEI during reconstructions of Lateglacial and Holocene palaeoenvironments in the Baltic Sea based on sedimentary records from the Gdansk Basin and the Gulf of Finland (Grigoriev *et al.* 2011; Virtasalo *et al.* 2014). The method is based on the estimate of behaviour-affinity of Cl and Br and a stable Cl/Br ratio is 230 in the water column and in pore waters of the Baltic Sea sediments (Shishkina *et al.* 1969); it is further based on the experimentally confirmed assumption that this ratio remains fairly stable during the sediment accumulation in freshwater environments. The Br-based salinity (S) was estimated using the empirical formula $S‰ = 0.115 + 1.80655 \times (Br‰ - 0.0046‰) \times 230$, which was modified from the Cl-based formula $S‰ = 0.115 + 1.80655\ Cl‰$ used by Snezhinsky (1951) and Lyahin (1994). The constant value of 0.0046‰ was determined as a regional background of Br concentration in the minerals of silty clay sediment accumulated in freshwater basins (Grigoriev *et al.* 2011).

For the 18GG-2t, 18MI-1t, 18MI-2t, 17KRG-1 and 17KRG-3 cores, the total organic carbon (TOC) content of sediments and loss on ignition (LOI) were determined (every 5 cm, using 1-cm-thick slices). For the primary sediment treatment, wet samples were dried at 90 °C and ground into a powder using an agate mortar. Samples were again dried at 90–100 °C and then placed in a desiccator. The TOC content of sediment was determined by the coulometric method using an AN-7529 analyser. To determine the LOI, the dried samples were ashed in a muffle furnace at 550 °C for 3 h and weighed; ashing was continued for approximately 2 h until a constant weight was reached. The resulting mass difference was calculated as a percentage value. According to Leipe *et al.* (2011) and Jensen *et al.* (2017), for the Baltic Sea sediments, the LOI provides a good estimate of the TOC content of the sediments.

For the sediment chronology, radiometric accelerator mass spectrometry (AMS) ^{14}C dating was performed on bulk sediment samples at the Center for Collective Use 'Laboratory of radiocarbon dating and electron microscopy' of the Institute of Geography of the Russian Academy of Sciences, and the Center for Applied Isotope Studies of the University of Georgia (USA). A total of 13 AMS ^{14}C dates for the 17GG-1t, 17KRG-3 and 18MI-1t cores were obtained (Table 2). All ^{14}C dates were calibrated by CALIB REV7.1.0 (Reimer *et al.* 2013) using the Intcal13.14c calibration curve. The calendar age (before present; BP = AD 1950) is represented as an average value within the 1σ confidence interval.

For the EGoF, the first calculation of reservoir effect was performed by specialists of the GTK based on joint investigations of the 09F40 core (Virtasalo *et al.* 2014). The age model was based on AMS ^{14}C dates and Pb distribution in the core. In the Baltic Sea, the Pb maxima

Table 2. Results of radiocarbon dating conducted at the Center for Collective Use 'Laboratory of radiocarbon dating and electron microscopy' of the Institute of Geography of the Russian Academy of Sciences and the Center for Applied Isotope Studies of the University of Georgia (USA). Radiocarbon ages were calibrated using Calib Rev. 7.1 and the Intcal13.14c calibration curve with a local reservoir age of *c.* +370 years.

Depth (cm)	Dated material	^{14}C age ±1σ (a BP)	Calibrated age (a BP, 1σ range)	Calibrated age mean with a local reservoir age +370 years (ka BP, 1σ range)
17KRG-3				
36–37	Bulk	1960±20	1884–1927	1.5
42–43	Bulk	1995±20	1903–1986	1.5
99–100	Bulk	3590±20	3853–3914	3.5
18MI-1t				
24–25	Bulk	1280±20	1184–1265	0.8
44–45	Bulk	5050±20	5746–5886	5.4
79–80	Bulk	6505±20	7420–7435	7.1
83–84	Bulk	8615±25	9535–9576	9.1
183–184	Bulk	15 540±35	18 748–18 847	18.4
17GG-1t				
9	Bulk	1420±20	1301–1331	0.9
12	Bulk	5620±20	6349–6368	6.0
57	Bulk	7540±25	8353–8386	8.0
60	Bulk	8240±25	9441–9478	9.1
90	Bulk	10 620±40	12 566–12 649	12.2

in the marine sediments for the last 2000 years have been well known in recent decades. These maxima are related to the atmospheric deposition peaks that occurred about 750 a BP ('medieval increase') and in the 1970s (Renberg *et al.* 2002; Zillén *et al.* 2012). This allowed an estimation of the reservoir effect of +350 years. The same approach was applied to this work. Thus, the AMS ^{14}C dating of the 18MI-1t core allows determination of the age of the sediment layer above the erosion surface at 24–25 cm as 1184–1207 a BP. The box-corer sampling confirmed that sedimentation in the core site is still continuing. The Pb distribution curve demonstrates peaks at the 22–24 and 4–6 cm horizons (Fig. 3). According to these data, the local reservoir effect for the 18MI 1t core can be estimated as +370 years. In this study, we present calibrated ages taking into account the abovementioned local reservoir effect as 'ka BP' (Table 3).

Magnetic susceptibility measurements were carried out on the nine sediment cores, apart from the 09F40 core, which was only used for comparison. One of the nine sediment cores, Core 17GG-1t, was additionally subjected to palaeomagnetic studies. Magnetic susceptibility was measured on the undisturbed surface of the core sections with a Kappameter KT-5 and/or MS2E surface sensor (Bartington, UK), at 6.5 and 2.5 cm horizons, respectively. During the MS2E measurements, the baseline drift correction was implemented to minimize a temperature-induced drift of the sensor and to eliminate this phenomenon from the data. The magnetic susceptibility values were automatically recalculated using Multisus software (Multisus version 2.44, 2006, for Windows 98/NT/2000/XP, Bartington Instruments Ltd).

Core 17GG-1t was sampled continuously with plastic cubes of approximately 8 cm^3. Since for the present study, only the first 2 m of the core were of interest, 51 oriented samples from the upper 200 cm of the core section were collected. Palaeomagnetic measurements were carried out at the Center for Geo-Environmental Research and Modeling (GEOMODEL), St. Petersburg State University. Measurements of natural remanent magnetization (NRM) were carried out with an SRM-755 SQUID magnetometer (2G Enterprises, USA). To remove the viscous remanent magnetization induced by the modern geomagnetic field, a stepwise alternating field (AF) demagnetization technique was applied to the 51 samples. The measurements were made in 14 steps of peak AFs from 5 to 100 mT (increments of 5 mT for the 5–30 mT peak AFs, and 10 mT for 30–100 mT peak AFs). The characteristic remanent magnetization (ChRM) with the maximum angular deviation (MAD) was estimated based on stepwise AF demagnetization results from 20 to 80 mT using (Kirschvink 1980) the Demagnetisation Analysis in Excel software (Sagnotti 2013). Due to the arbitrary horizontal orientation of the core, the magnetic declination of the geomagnetic field was further considered as a relative alteration in the core due to its arbitrary horizontal orientation during the retrival.

Measurements of anisotropy of magnetic susceptibility in the 17GG-1t core (upper 260 cm) were performed on 119 samples collected continuously using the spinning specimen method with an MFK1-FA Kappabridge (Agico, Czech Republic) installed at GEOMODEL. Three successive rotations around three mutually perpendicular axes were carried out. One bulk magnetic susceptibility value was measured along one axis, and the full susceptibility tensor was determined based on the measurements. Calculation of the anisotropy tensor represented by the maximum, intermediate and minimum principal susceptibilities (k_{max}, k_{int} and k_{min}, respectively) and their respective orientation angles was performed using AGICO software (Brno, Czech Republic). The orientation angles were given with respect to sample coordinates (x, y) and geographical coordinates (z). The anisotropy of magnetic susceptibility measurements were carried out before the demagnetization procedures for the relevant samples. The data on the anisotropy of magnetic susceptibility can serve as a useful tool to reconstruct the depositional environment (Dudzisz *et al.* 2016) because the minimum values along the vertical axis indicate calm sedimentary conditions.

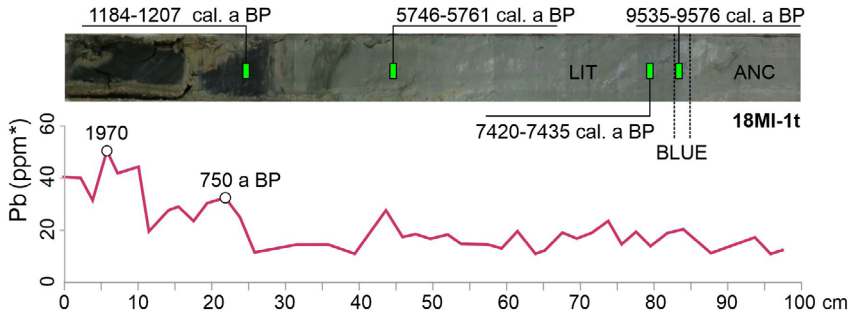

Fig. 3. Age model based on AMS ^{14}C dates and Pb concentration in the 18MI-1t sediment core. ANC = Ancylus Lake deposits; BLUE = 'blue clays'; LIT = Littorina Sea deposits.

Table 3. The acoustic and lithostratigraphy in the EGoF.

Acoustic stratigraphy in the eastern Gulf of Finland (Spiridonov *et al.* 2007; Ryabchuk *et al.* 2020b)				Acoustic unit interpretation used in this paper	Typical acoustic section
Acoustic unit	Description	Lithology	Interpretation (the Baltic Sea stages)		
pLIT+LIT	Quasihorizontal in-phase axes of variable amplitude (usually higher than in ANC unit) reflections.	Olive-grey silty clays with a high content of black dispersed organic material; in some sedimentary basins gas-saturated.	The marine Littorina and post-Littorina mud	AU1 (Figs 4, 6, 8)	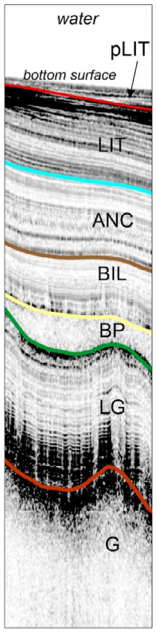
ANC	The chaotic reflections fade to top superimposed on quasihorizontal in-phase axes of variable amplitude reflections. The boundary of this unit and AU1 can't be distinguished clearly sometimes due to its similarity and lack of nonconformity.	Grey to brownish-grey soft clays with the presence of distinct black hydrotroillite inclusions, which are grouped into 'chains' (0.1–1.5 cm thick), and which form so-called 'hydrotroillite horizons', enriched with these inclusions.	The Holocene Ancylus Lake	AU2 (Figs 4, 6, 8)	
BIL	The parallel rhythmic reflections with in-phase axes of varying amplitudes in the seismic-reflection profiles that conform with the surface of the underlying acoustic unit. Amplitudes of reflections are high in the base of the acoustic unit with attenuation to the top of it. Frequencies of signals are changing from low to high,	Transition from thin-laminated (less than 1 mm) to homogenous brownish clays, with alternating brown, red-brown, and grey bands.	Distal facies of the Baltic Ice Lake	AU3 (Figs 4, 6, 8)	
BP	The acoustic transparent zone that lacks reflections; observed locally in the western part of EGoF.	Dense homogenous clay enriched with sand.	Proximal facies of the Baltic Ice Lake		
LG	Structure of the record is similar to AU3, but has a lower frequency and higher amplitudes of the reflected signal and lower position in cross-section.	Varved clays are rhythmic (varve thickness from a few mm to 10–20 cm), with laminations of alternately finer and coarser grey clays and brown silt, reflecting seasonal sedimentation.	Proximal facies of the Baltic Ice Lake	AU4 (Figs 4, 6, 8)	
FG	The zone with contrast interfaces that are characterized by acoustic transparent reflections or reflections with transversal in-phase axes in the seismic cross-section; locally observed; fill the depressions; underlain by till.	Sands and sands with gravel and pebbles.	Glacifluvial deposits		
G	The acoustic transparent zone that lacks reflections. Discontinuous high-amplitude reflections lacking an explicit in-phase correlation at the upper boundary	Very dense brownish sandy clays (clayey sands), comprised of up to 15–20% silt, while the coarse material content (including boulders with traces of glacial striation) reaches 30%.	Last Glacial till	AU5 (Figs 4, 6, 8)	

Results

Acoustic units

In this paper, we studied three sedimentary basins (Fig. 1) located: (i) east of Gogland Island (8W) (Figs 4, 5); (ii) west of Moshchny Island (8E) (Figs 6, 7); and (iii) north of Shepelevo Cape (2) (Figs 8, 9). Results of the previous research on sedimentary basin 3 (located south of the Berezovye Islands) (Virtasalo *et al.* 2014) were used in this study for comparison.

The sub-bottom profiling, which preceded sediment sampling, revealed five AUs (AU5 – bottom to AU1 – top) within every zone where sampling was planned. AU5, the acoustic transparent zone showed a lack of reflection, and discontinuous high-amplitude reflections lacking explicit in-phase correlation at the upper boundary. AU4 and AU3 displayed parallel rhythmic reflections with in-phase axes of varying amplitudes in the seismic-reflection profiles that conformed with the surface of the underlying acoustic unit; there was furthermore a distinct boundary between them. The upper contact of AU3 was indicated by a sharp discontinuous acoustic boundary. AU1 and AU2 had distinct subhorizontal in-phase axes of variable amplitude reflections. Within the sedimentary basins 8W and 8E, they were separated by the distinct acoustic boundary. Since a different acoustic method was applied in sedimentary basin 2, it was not possible to distinguish AU1 from AU2. Thus, the results for AU1 and AU2 were disregarded.

Results of sediment sampling

Western part of sedimentary basin 8W east of Gogland Island (sites 17GG-1t, 18GG-1t and 18GG-2t). – Cores 17GG-1t, 18GG-1t and 18GG-2t (Figs 4, 5, S1) were taken in the western part of sedimentary basin 8W (Fig. 1), on the slopes of submarine moraine ridges at a water depth of 63.75, 61.5 and 62.25 m, respectively (Fig. 4).

The upper part of AU3 was recovered in the 17GG-1t and 18GG-2t cores, which were represented by homogenous brownish-grey clays with pronounced colour banding (core intervals 465–239 and 267–262 cm,

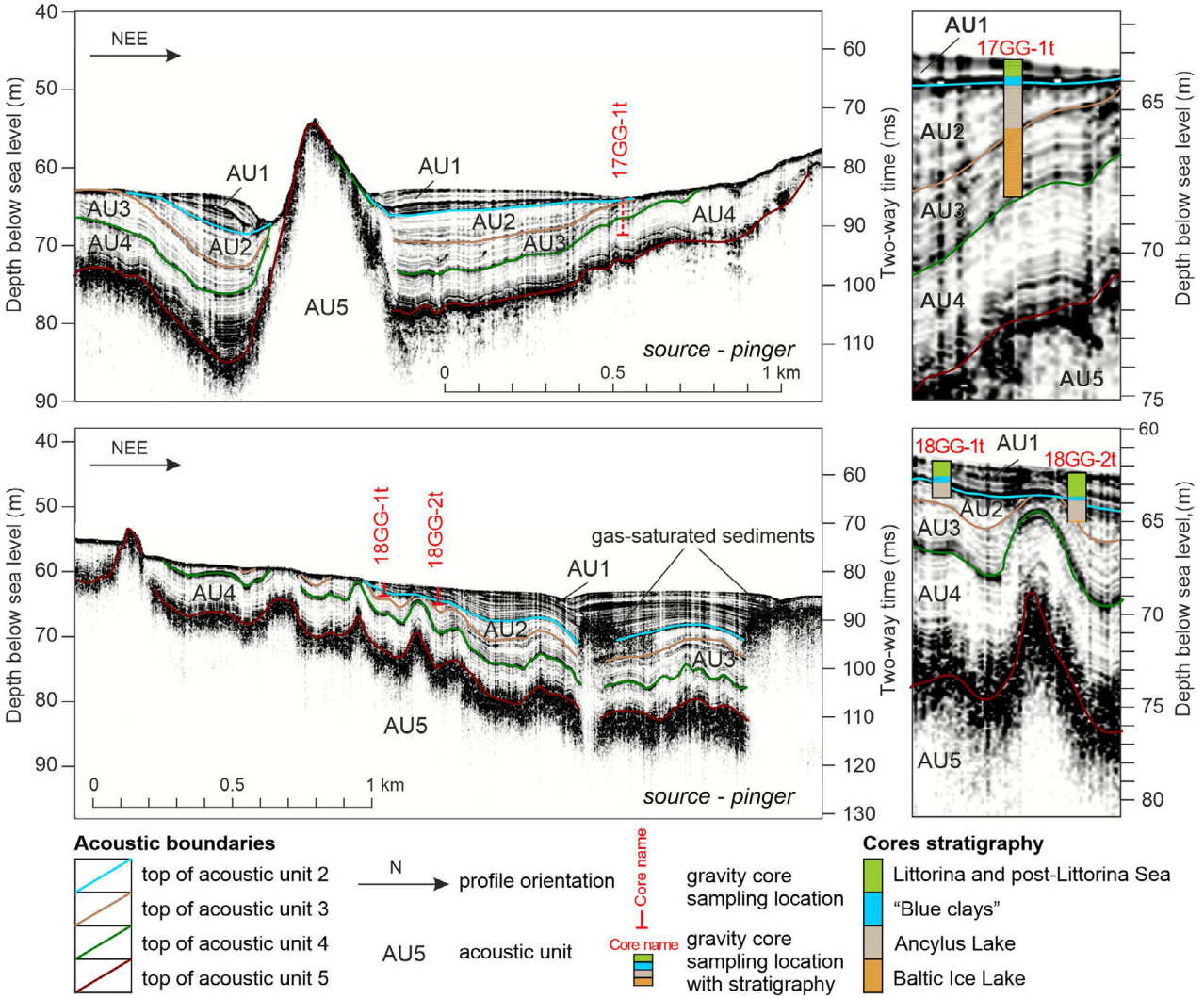

Fig. 4. Cores 17GG-1t, 18GG-1t and 18GG-2t on the acoustic profiles. AU1 = Littorina Sea deposits; AU2 = Ancylus Lake deposits; AU3 = homogenous clays of the Baltic Ice Lake; AU4 = varved clays; AU5 = Last Glacial till. EdgeTech 3300-HM sub-bottom profiler (pinger type system).

respectively; Figs 2, 5A, B). Within the intervals, the average grain-size fraction <0.005 mm was 79.8%. The grain-size parameters were relatively stable along these core intervals (Fig. 5A, B). The distributions of Si, K and Zr changed slightly corresponding to grain-size distribution, while the variability of most of the other measured elements (e.g. Mn and Br) was low in the lower core section and increased in the upper part of the core. The estimated palaeosalinity was 1.1–1.5‰. In the 18GG-2t core, the average LOI value and TOC content were 4.7 and 0.76%, respectively (Fig. 5B). In the 17GG-1t core, an abrupt change in the grain-size distribution with an increase in silt fraction occurred at the upper boundary of this sediment unit (at a core depth of 239 cm; Fig. 5A). However, a sand-rich interlayer indicating an erosion event was not present.

AU2 was recovered in cores 17GG-1t (core depth 239–91 cm), 18GG-2t (core depth 262–151 cm) and 18GG-1t (core depth 198–117 cm), with the unit thickness being 144, 111 and 81 cm, respectively (Figs 2, 5). Deposits were represented by brownish-grey clays. Layers enriched with distinct black hydrotroillite inclusions and spherical hydrotroillite bundles with a diameter of 0.1–1.5 cm were generally observed near the upper and lower boundaries of the unit. Grain-size composition of these deposits was coarser than sediments of the underlying unit. In the 17GG-1t core, the interval 216–116 cm was dominated by clays (Fig. 5A). However, the content of the clay fraction <0.005 mm was slightly lower (70.1–84.3%, averaging 73.8%) when compared with sediments of underlying sediments of AU3 (where average content of clay particles was 79.8%). The silt fraction varied in the range of 11.0–25.7% (average 17.4%) and the sand fraction was less represented (0–6.5%, average 5.0%). Coarser layers (silty clays) were observed within the core intervals 239–227, 224–223 and 222–217 cm. The clay, silt

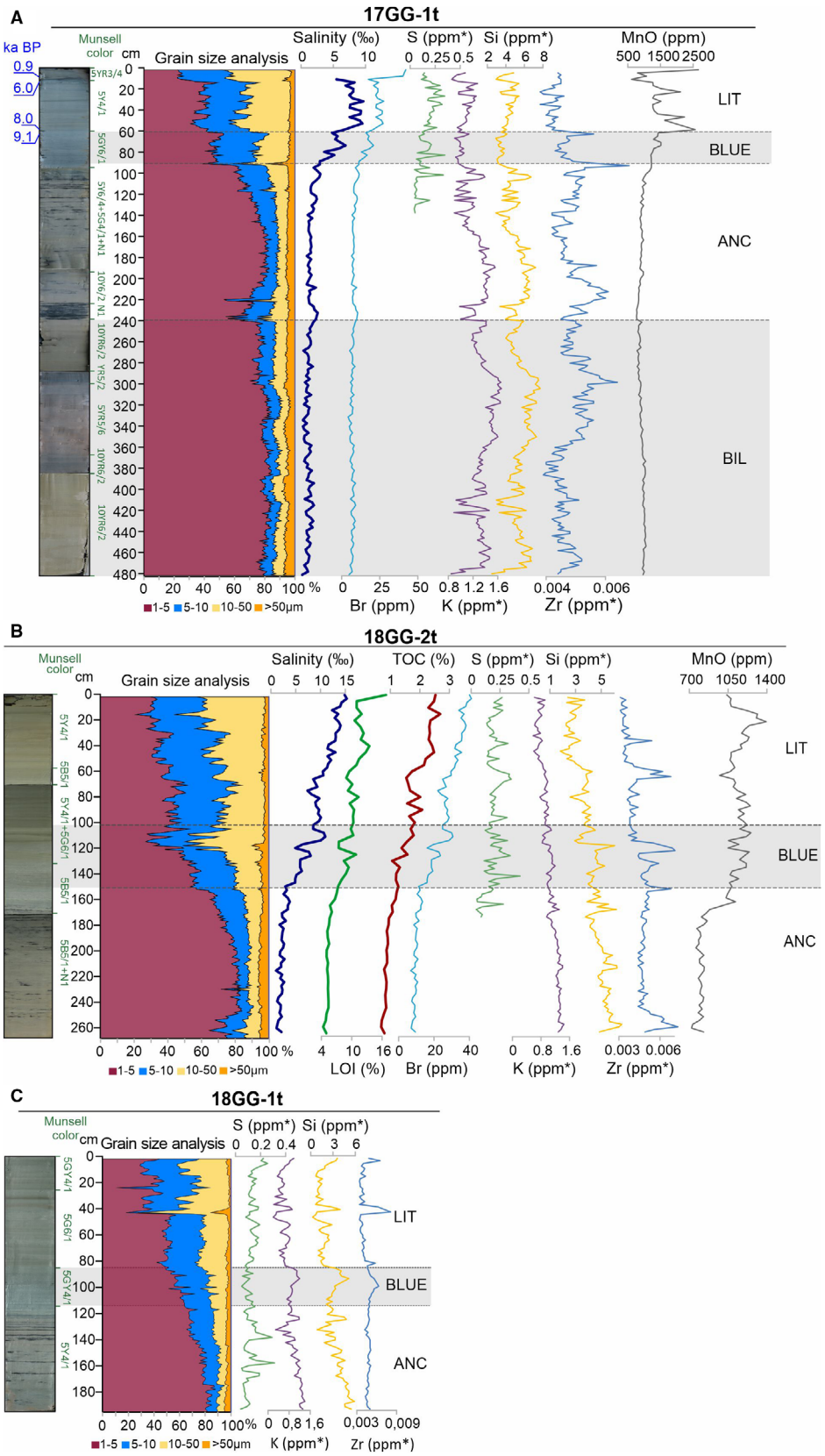

Fig. 5. Photographs, grain-size distributions and some geochemical parameters of the 17GG-1t, 18GG-1t and 18GG-2t cores. BIL = Baltic Ice Lake deposits; ANC = Ancylus Lake deposits; BLUE = 'blue clays'; LIT = Littorina Sea deposits. Asterisk denotes results from XRF-scanner.

and sand fractions were 53.5–69.6% (average 64.4%), 24.0–41.4% (average 31.0%) and 3.3–6.4% (average 4.6%), respectively (Fig. S1). A gradual increase of clay (from 64 to 82%) was observed at core depth 239–170 cm, whilst a decrease in clay (from 82 to 62%) was observed in the upper part of the core interval 170–91 cm (Fig. 5A). Similar trends of gradual increasing, followed by gradual decreasing of clay content were identified in deposits in the 18GG-2t and 18GG-1t cores (Fig. 5B, C).

Distributions of Si, K and Zr in the 17GG-1t core were slightly more changeable than in the underlying sediment unit, with Mn content remaining low, and S content being detectable in the upper part of sediment unit (Fig. 5A). Br content and estimated palaeosalinity (1.1–1.5‰) and their respective variabilities, were found to be low. A slight increase in palaeosalinity (up to 2.5–3‰) was recorded within the upper 20 cm of the described sediment unit (Fig. 5A, B). Distributions of LOI value and TOC content within this sediment unit were slightly higher compared to underlying sediments of AU3 (5.5 and 0.9%, respectively; Fig. 5B).

In the 17GG-1t core, the upper contact of the described deposits was marked by a 1-cm-thick silty clay layer enriched with a sand fraction (38.7% clay, 42.0% silt and 19.3% sand fractions). Vertical distribution of Zr demonstrated a sharp increase in content within the silty clay layer, indicating an increase in clastic sediment input (Fig. 5A). AMS ^{14}C dating of the layer (17GG-1t core, 90–91 cm) demonstrated an age of 12.2 ka BP (Table 2).

In all three studied cores from the western part of sedimentary basin 8W, sediments of the described unit were overlain by a thin, lithologically specific layer of so-called 'blue clays': in the 17GG-1t (core depth 91–60 cm; Fig. 5A); 18GG-1t (core depth 117–84 cm; Fig. 5C); and 18GG-2t (core depth 151–130 cm; Fig. 5B) cores, with thicknesses of 34, 32 and 30 cm, respectively. The grain-size distribution of the

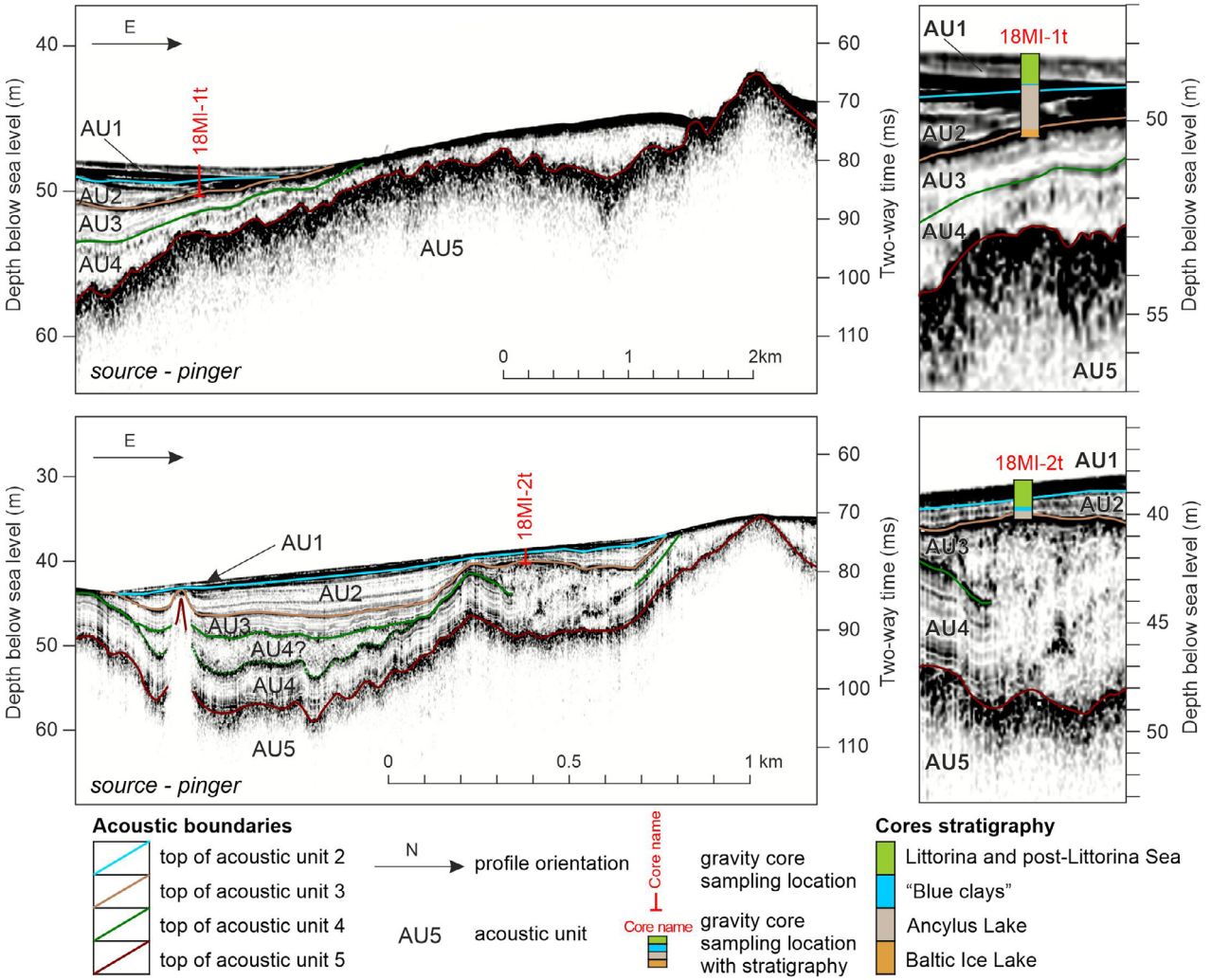

Fig. 6. Location of the 18-MI-1t and 18-MI-2t cores on the acoustic profiles. AU1 = Littorina Sea deposits; AU2 = Ancylus Lake deposits; AU3 = homogenous clays of the Baltic Ice Lake; AU4 = varved clays; AU5 = Last Glacial till. EdgeTech 3300-HM sub-bottom profiler (pinger type system).

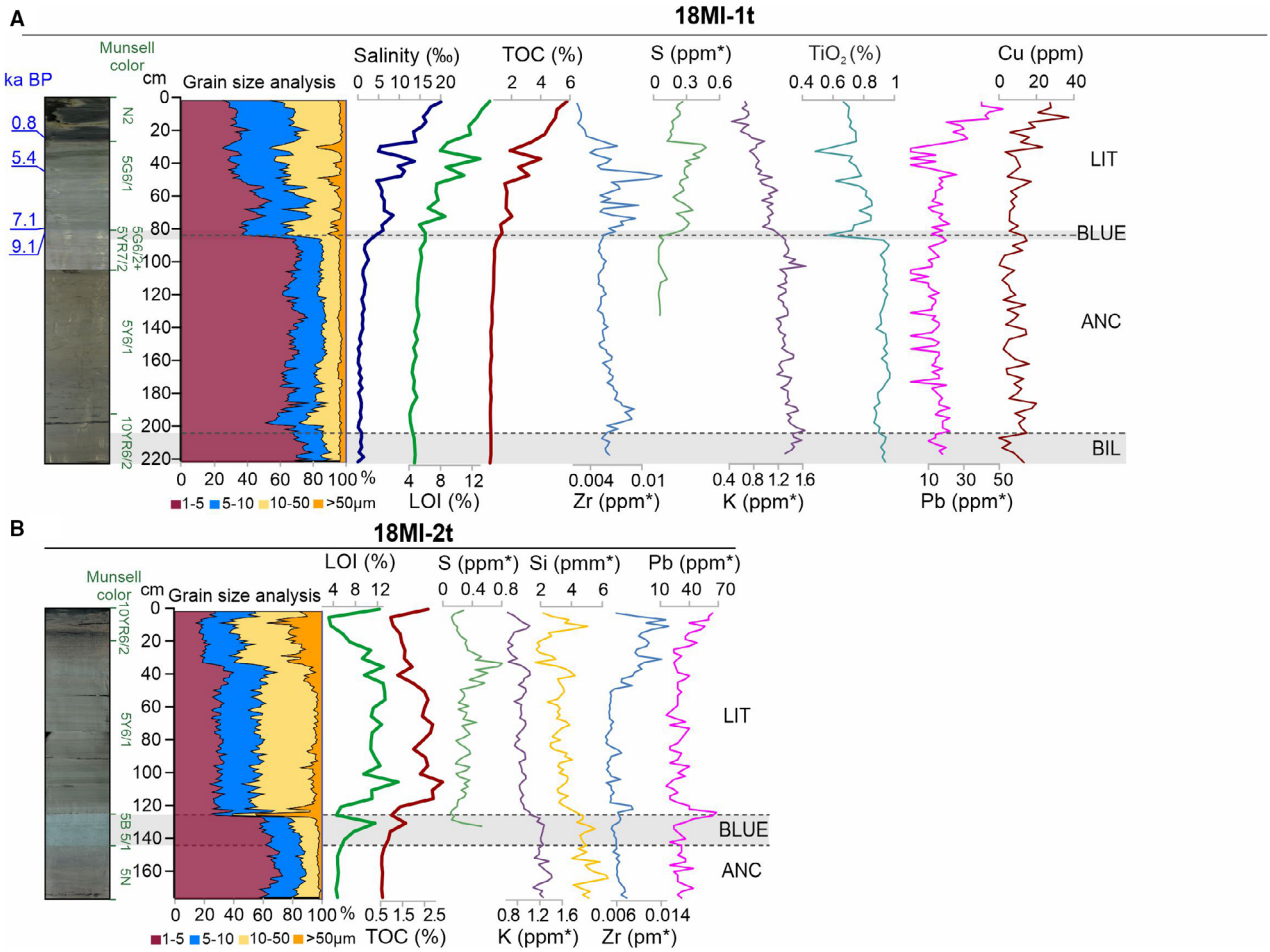

Fig. 7. Photographs, grain-size distributions and some geochemical parameters of the 18MI-1t and 18MI-2t cores. BIL = Baltic Ice Lake deposits; ANC = Ancylus Lake deposits; BLUE = 'blue clays'; LIT = Littorina Sea deposits. Asterisk denotes results from XRF-scanner.

sediments within this layer shifted towards the silt fraction. 'Blue clays' were represented by the bluish-grey clayey silts and silty clays (Fig. S1).

Within the described stratigraphical unit, a significant increase in LOI value (up to 8.4%) and TOC (up to 1.2%) in the 18GG-2t core (Fig. 5B); Mn and Br content in the 17GG-1t and 18GG-2t cores (Fig. 5A, B), as well as Si, K and S content in the 18GG-2t and 18GG-1t cores, was observed (Fig. 5B, C). The values of estimated palaeosalinity increased stepwise from 2 to 7‰ (Fig. 5A, B). AMS ^{14}C dating of the 'blue clays' layer (17GG-1t core, 60–61 cm) determined the age of the sediments as 9.1 ka BP (Table 2). Since they form a relatively thin (about 30 cm) layer, 'blue clays' could not be identified on SBP profiles.

The uppermost sediment unit (AU1; core depth 60–0 cm in 17GG-1t, 84–0 cm in 18GG-1t and 103–0 cm in 18GG-2t) was represented by olive-grey silty clays. It is noteworthy that, in contrast to other stratigraphical units, the structure and lithology of this unit varied significantly in the three studied cores. A silt fraction dominated the sediments (47.4–65.1%, average 58.4%), whereas the clay fraction decreased compared to the underlying layers (31.1–49.2%, average 39.2%). The sand admixture remained relatively low (2.6–8.0%, average 3.4%) (Fig. 5A–C).

In the 17GG-1t and 18GG-1t cores, the lowest 30 cm of the uppermost sediment unit was represented by the olive-grey thin-laminated (less than 1 mm thick) silty clays and clayey silts (Fig. 5A, C). The average clay, silt and sand fractions were 49.9, 47.7 and 2.4%, respectively. Lamination (expressed by colour) was very distinct and was not disturbed by bioturbation. In the 17GG-1t core, the horizon 57–58 cm was dated to 8.0 ka BP (Table 2). In the 18GG-2t core, core interval 130–103 cm was represented by the alternation of thin-laminated and homogenous bluish-grey clayey silts. Sediments in this part of the unit were coarser (average clay, silt and sand fractions were 38.0, 57.8 and 4.38%, respectively). It is likely that the sediments had been disturbed by submarine landslides (Fig. 5C). In the

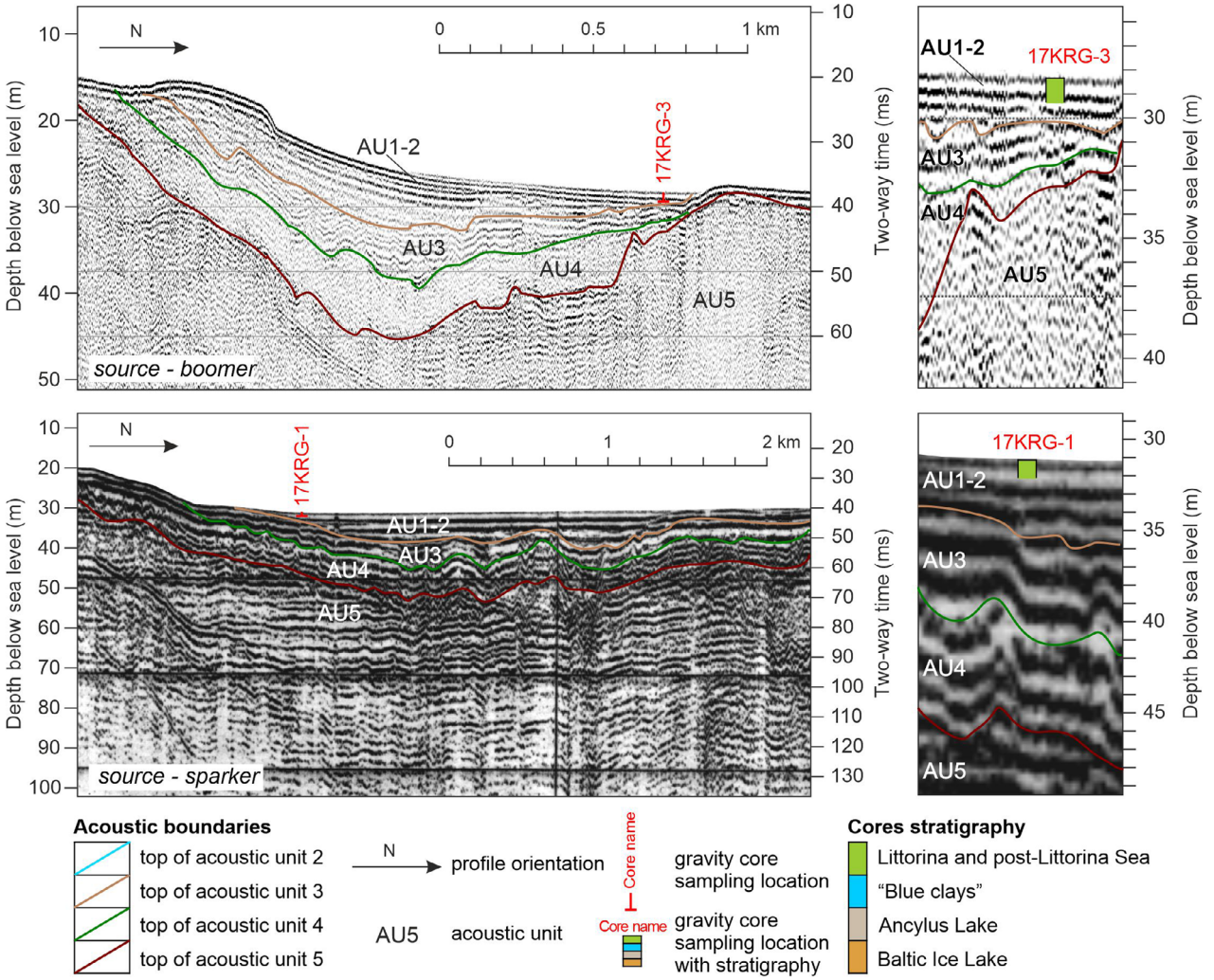

Fig. 8. Location of the 17KRG-1 and 17KRG-3 cores on the acoustic profiles. AU1 = Littorina Sea deposits; AU2 = Ancylus Lake deposits; AU3 = homogenous clays of the Baltic Ice Lake; AU4 = varved clays; AU5 = Last Glacial till. GEONT-HRP 'Spektr-Geophysika' Ltd. sub-bottom profiler (boomer and sparker type system).

18GG-2t core, the interval 103–80 cm was distinctly thin-laminated (thickness of lamination is less than 1 mm).

In the 17GG-1t core, the laminated sediments within the interval 57–27 cm were overlain by bioturbated olive-grey clayey silt (27–10 cm interval; Fig. 5A). Sediments at 12–13 cm core depth were dated to 6.0 ka BP (Table 2). At the 10-cm core depth, a sharp change in lithology, colour, and grain-size distribution was observed, indicating erosion contact. Sediments above the erosion layer were represented by brownish silt with patchy structure caused by the presence of black dispersed organic matter (Fig. 5A). Dating of deposits at the 9-cm core depth showed an age of 0.9 ka BP (Table 2).

Laminated sediments of the 18GG-1t core (interval 60–42 cm) were interrupted by a distinct erosion layer at 41–42 cm (sand fraction content increases to 10–15%). Above the erosion layer, sediments were represented by the dark greenish-grey, partly laminated clayey silts (Fig. 5C). The thickness of the deposits representing AU1 in the 18GG-2t core was 130 cm. Laminated silty clay deposits of the lower part of the unit were gradually replaced by partly laminated and homogenous bioturbated sediments (Fig. 5B).

The lower contact of the AU1 deposits was marked by a sharp increase in LOI value (up to 10.6%) and TOC (up to 2.0%) content in the 18GG-2t core (Fig. 5B), as well as S, Si, K, Mn and Br content in the 17GG-1t core (Fig. 5A). The erosion layers were found to be enriched with Zr (Fig. 5A–C).

The uppermost interval of the 17GG-1t core (11–0 cm) differed from the underlying sediments in geochemical parameters. The calculated palaeosalinity decreased dramatically (to 5.3‰; Fig. 5A). At the same time, in the 18GG-2t core, calculated palaeosalinity increased from 6 to 14‰ (Fig. 5B). In the 17GG-1t core, three

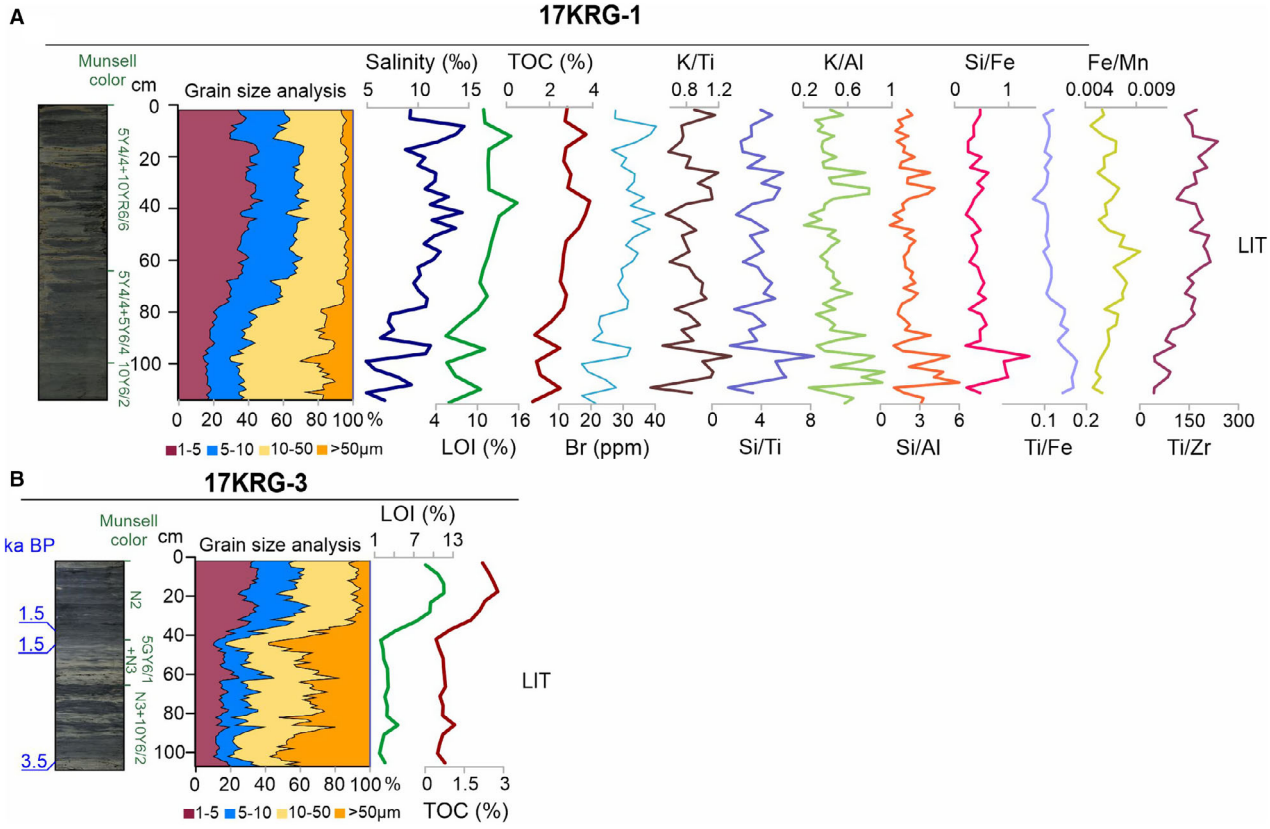

Fig. 9. Photographs, grain-size distributions and some geochemical parameters of the 17KRG-1 and 17KRG-3 cores. LIT = Littorina Sea deposits.

maxima of palaeosalinity could be identified within the time interval from 6.0 to 8.0 ka BP: at the 51–52 cm (9.5‰), 39–43 cm (9.2‰) and 30–31 cm (9.6‰) horizons, with the amplitude of palaeosalinity variation being about 2‰ (Fig. 5A).

Northeastern part of sedimentary basin 8E, west of Sommers Island (sites 17SOM-1, 17SOM-2). – The 17SOM-1 and 17SOM-2 cores (Figs 2, S2, Table 1) were taken in the northeastern part of the Gogland sedimentary basin at water depths of 63.00 m and 63.75 m, respectively. The core sections are represented by olive-grey clayey silts. In the lower part of the 17SOM-2 core (interval 152–133 cm), a 'blue clay' layer was recovered. Above 133 cm, the grain-size distribution demonstrated an increase in silty fraction. The lower intervals of both cores (142–114 cm in 17SOM-1 core and 129–118 cm in 17SOM-2 core) were characterized by a distinct thin lamination and by the absence of bioturbation. In the 17SOM-1 core, at 114–115 and 92–93 cm horizons, there were erosion surfaces marked by a sharp increase in sand fraction, and by maxima in Zr content. Br content and calculated palaeosalinity increased throughout the core section from around 6 or 8–14‰ and from around 6 to 10 and ranging up to 14 ‰ in the 17SOM-1 and 17SOM-2 cores, respectively (Fig. S2).

Eastern part of sedimentary basin 8E near Moshchny Island (sites 18MI-1t, 18MI-2t). – Sampling sites 18MI-1t and 18MI-2t (Figs 6, 7, S3) were located in the eastern part of the Gogland sedimentary basin, at water depths of 48 m and 38.25 m, respectively. The location of sampling sites was chosen based on SBP data previously obtained (Ryabchuk *et al.* 2020b) from the gentle slopes of submarine ridges (Fig. 6).

According to the box-corer sampling at the 18MI-1t and 18MI-2t sites, surface sediments (0.5 cm) are represented by oxidized brownish silty clays with a high sand fraction content. At the 5 cm core depth, almost-dissolved Fe-Mn concretions were observed. Sediments at box-core interval 5-40 cm are represented by black colour silty clays with a significant amount of sand particles (Fig.7).

The 18MI-1t core recovered AU3 sediments (218–204 cm interval) represented by brownish silty clays and clays (clay fraction content varied from 68 to 79.6%, average 73.0%) with colour banding (Fig. 7A).

In the 18MI-1t core, at a 204-cm core depth, these deposits were observed to be replaced by the sediment unit (204–85 cm) represented by brownish olive-grey silty clays without a sand-enriched layer (clay fraction content is 51.1–77.7%, average 66.8%). At the 108–133 and 187–196 cm intervals, a large number of lenses, nodules, and spots of authigenic sulphites were observed ('lower'

and 'upper hydrotroillite horizons', respectively). Both grain size and distribution of chemical components did not change significantly upcore, although a slight upcore increase in clay content was traced. Within the 'lower hydrotroillite horizon', relatively high concentrations of S, Pb and Cu and lower content of Ti and K were registered (Fig. 7A). AMS ^{14}C dating of the 18MI-1t core (core depth 183–184 cm) provided the age of the sediments of 18.4 ka BP (Table 2). The 18MI-2t core section recovered only the upper part of AU2 (core depth 177–144 cm; Fig. 7B); the upper boundary of AU2 deposits was indicated by the change in composition of grain size of the sediments in both the 18MI-1t and 18MI-2t cores. The average LOI value and TOC content in the AU2 sediments of both cores were 4.8 and 0.6%, respectively, with a slightly increasing trend from bottom to top of the core (Figs 7A, B, S3).

The 'blue clays' layer was observed in both cores: as a very thin (2 cm) layer in the 18MI-1t core (core depth 85–83 cm), and as a relatively thick (19 cm) layer in the 18MI-2t core (core depth 144–125 cm). The layer was represented by silty clays, with a clay fraction content of 56.5–69% (average 62.8%). At the upper 'blue clays' boundary, a sharp increase in sand fraction (up to 45.2%) was observed. The transition to the 'blue clays' layer above the core depths 85 cm (core 18MI-1t) and 144 cm (core 18MI-2t), was accompanied by a sharp increase in LOI value and TOC content (up to 6.0 and 1.0% in 'blue clays' and up to 14.2 and 5.8% in olive-grey silty clay, respectively) (Fig. 7A, B). Calculated salinity also increased. Sediments from the 'blue clays' layer in the 18MI-1 core (83–85 cm) were dated to 9.1 ka BP (Table 2).

In the 18MI-1t core, the transitional 'blue clays' layer was overlain by olive-grey bioturbated (83–30 cm interval) and dark olive-grey laminated (0–30 cm interval) clayey silts. Grain-size composition of deposits from the core interval 83–0 cm varied throughout the core (clay fraction content ranges from 24.7 to 54.8%, average 37.1%). Six sand-enriched layers with average coarse sand fraction content of 5.4% were also distinguished. The sand fraction in the layers was as follows: up to 11% (80–81 cm); up to 9.3% (77–78 cm); up to 9.3% (75–76 cm); up to 8.4% (66–67 cm); up to 16.1% (47–48 cm); and up to 18.0% (29–30 cm). Erosion surfaces were also marked by an increase in Zr content (Fig. 7A). The uppermost sediment unit deposits were dated right above the lower unit contact (79–80 cm – 7.1 ka BP) and above the two upper erosion layers: 44–45 cm – 5.4 ka BP and 24–25 cm – 0.8 ka BP (Table 2).

In the 18MI-2t core, erosion layers were not pronounced. However, based on the grain-size composition, geochemistry, and lithological features, three contacts could be assigned (Fig. 7B). The average clay fractions in the lower (125–33 cm), medium (33–6 cm) and upper (6–0 cm) intervals were 30.5, 19.2 and 24.2%, respectively.

In the upper part of cores, the content of heavy metals tended to increase. Distribution of LOI value and TOC content (Fig. 7A, B), as well as calculated palaeosalinity, showed a distinct increasing trend (from 1.6‰ for palaeosalinity in the bottom layer to 20‰ near the upper boundary), with the data indicating minimal values for palaeosalinity within the erosion layers (Fig. 7A).

Western part of sedimentary basin 2 (sites 17KRG-1, 17KRG-3). – The 17KRG-1 and 17KRG-3 cores (Figs 2, 8, 9, S4) from the easternmost shallow-water sedimentary basin at 31 and 27 m depths, respectively, recovered the upper section of AU1. Deposits of both the 17KRG-1 and 17KRG-3 cores were represented by silty sands and clayey silts (with an average clay fraction of 33 and 20.7%, respectively; Fig. 9A, B). They were partly thick-laminated (thickness of layers 1–2 cm) due to alternation of dark olive-grey and brownish sediments. The sediment sections were bioturbated, and there were no distinct sand-enriched layers. However, in the cores, two intervals with different grain-size compositions could be distinguished. It was noteworthy that the upper layer was dominated by a finer fraction than the lower one. Results of box-corer sampling indicate that the upper layer (0–3 cm) was represented by light brown silt with rare sand admixture, while the lower interval (3–15 cm) had dark grey clayey silt with numerous traces of benthic fauna. The lower part of the sediment core (73–114 and 37–106 cm intervals in 17KRG-1 and 17KRG-3 cores, respectively) was represented by sandy silts and silty sands. The grain-size distributions in the 17KRG-1 and 17KRG-3 cores were as follows: 18.7 and 15.3% of clays, 65.2 and 45.6% of silts, 16.2 and 39.1% of sands, respectively. Grain-size parameters of the uppermost intervals of both cores (73–0 and 37–0 cm intervals in 17KRG-1 and 17KRG-3 cores, respectively) demonstrated a significant shift towards the finer fraction – the average clay fraction increased up to 37.6 and 30.9%, respectively. In contrast, the average sand fraction contents dropped to 9.6 and 5.1%, respectively. Deposits of these intervals were classified as clayey silts (Fig. 9A, B).

Distribution of chemical elements throughout the 17KRG-1 and 17KRG-3 cores corresponded to the grain-size distribution in the sediments. In the 17KRG-1 core, the ratios of K/Ti, Si/Ti, K/Al, Si/Al, Si/Fe and Ti/Fe decrease and the ratios of Fe/Mn and Ti/Zr increase with an increase in clay fraction (Fig. 9A). In the upper part of the Littorina marine sediments, an increase in the majority of heavy metals content was observed. Br concentration and calculated salinity also increased upcore (from 6 to 14‰) and decreased dramatically within the uppermost 4 cm (Fig. 9A). In the 17KRG-3 core, the lower core section layer (99–100 cm interval),

and sediments both below and above the interval of sharp grain-size composition change (42–43 and 36–37 cm intervals), were dated. The ages obtained for the samples were 3.5 and 1.5 ka BP (Table 2).

Magnetic susceptibility and palaeomagnetic measurements

The magnetic susceptibility measurements were performed on all but the 09F40 core; six cores with notable susceptibility were then chosen for further analysis (Figs 10, 11). In the 17SOM-1, 17SOM-2 and 17KRG-1 cores, the magnetic susceptibility of AU1 was close to zero. While the magnetic susceptibility in AU1 was in the range of $0.1–0.15\times10^{-3}$ SI, sediments of AU2 had higher values ($0.2–0.3\times10^{-3}$ SI). The latter increased downcore, with maximum values in the lowest part of the unit. Several magnetic susceptibility peaks were sporadically distributed in different sediment units. They usually corresponded to sand layers and to intervals with the presence of hydrotroillite in the sediments.

The results of the palaeomagnetic studies in the 17GG-1t core are presented in Fig. 11. The interval 0–100 cm showed relatively low NRM intensity, around 10^{-4}–10^{-3} A m^{-1} (7.5×10^{-4} A m^{-1} on average). It then rose to 10^{-2} A m^{-1} (3×10^{-2} A m^{-1} on average) and then remained constant. At the 107-cm horizon, a sharp increase in the NRM intensity up to ~0.1 A m^{-1} was observed. It coincided with a peak in magnetic susceptibility and can be explained by the hydrotroillite interlayers at this depth.

In the upper 200 cm of the 17GG-1t core, the ChRM was estimated throughout the core section. At the 44.5-cm horizon, a negative inclination obtained during the NRM measurements was generally demagnetized by AF and then became positive. The interval was represented by the laminated unbioturbated sediments. From this depth and downcore, from 73 to 100 cm, the ChRM was accompanied by extremely high MAD, which indicates difficulties in defining a stable component of remanent magnetization. The MAD is a measure of precision and can be used to assess the quality of calculated ChRM data (Kirschvink 1980). From 100 cm, the demagnetization pattern and, consequently, the accuracy of the ChRM calculations changed sharply. The MAD reduced to well below 5° in most cases.

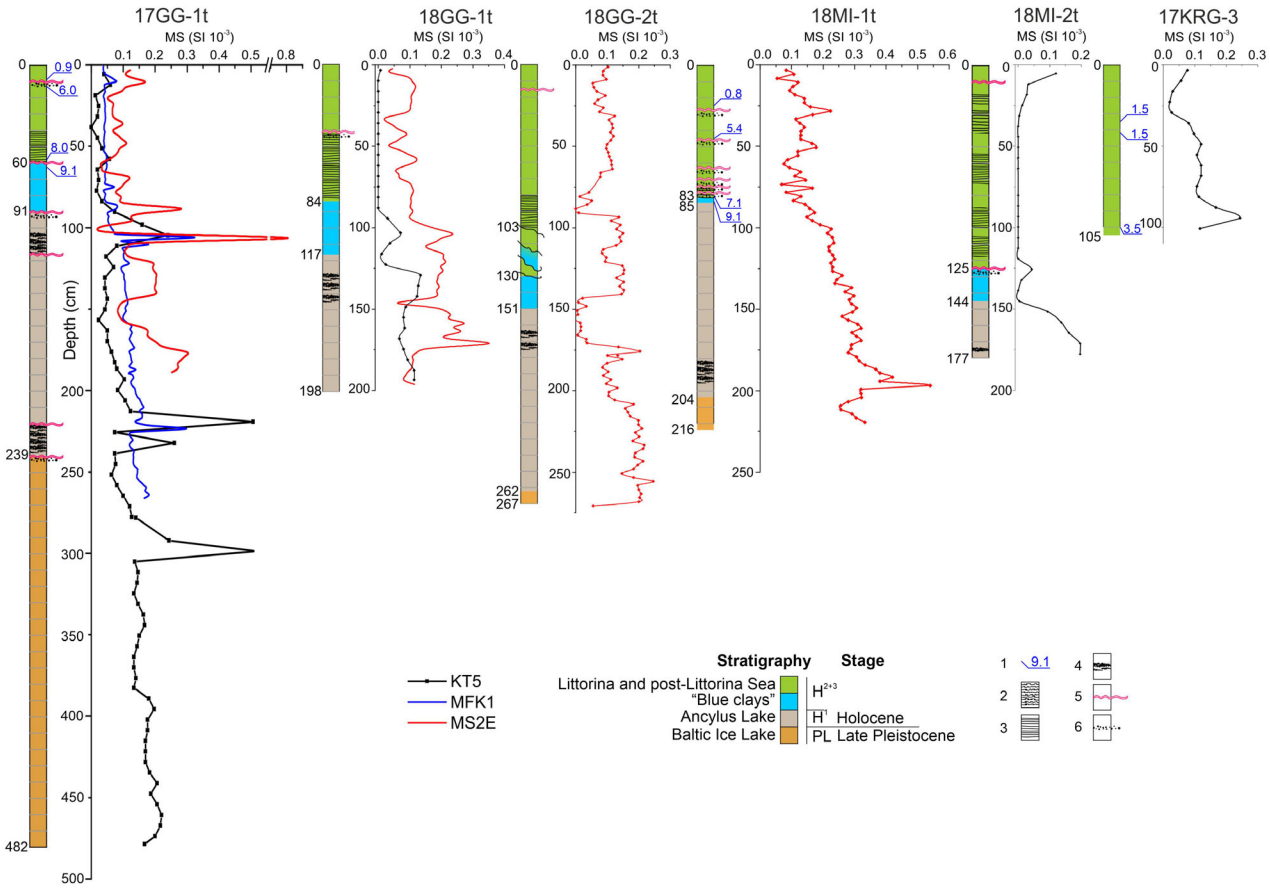

Fig. 10. Lithology and magnetic susceptibility (MS) of cores 17GG-1t, 18GG-1t, 18GG-2t, 18MI-1t, 18MI-2t and 17KRG-3. Data on magnetic susceptibility are obtained with different kappameters: dark blue is MFK1-AF, red is MS2E and black is KT-5.

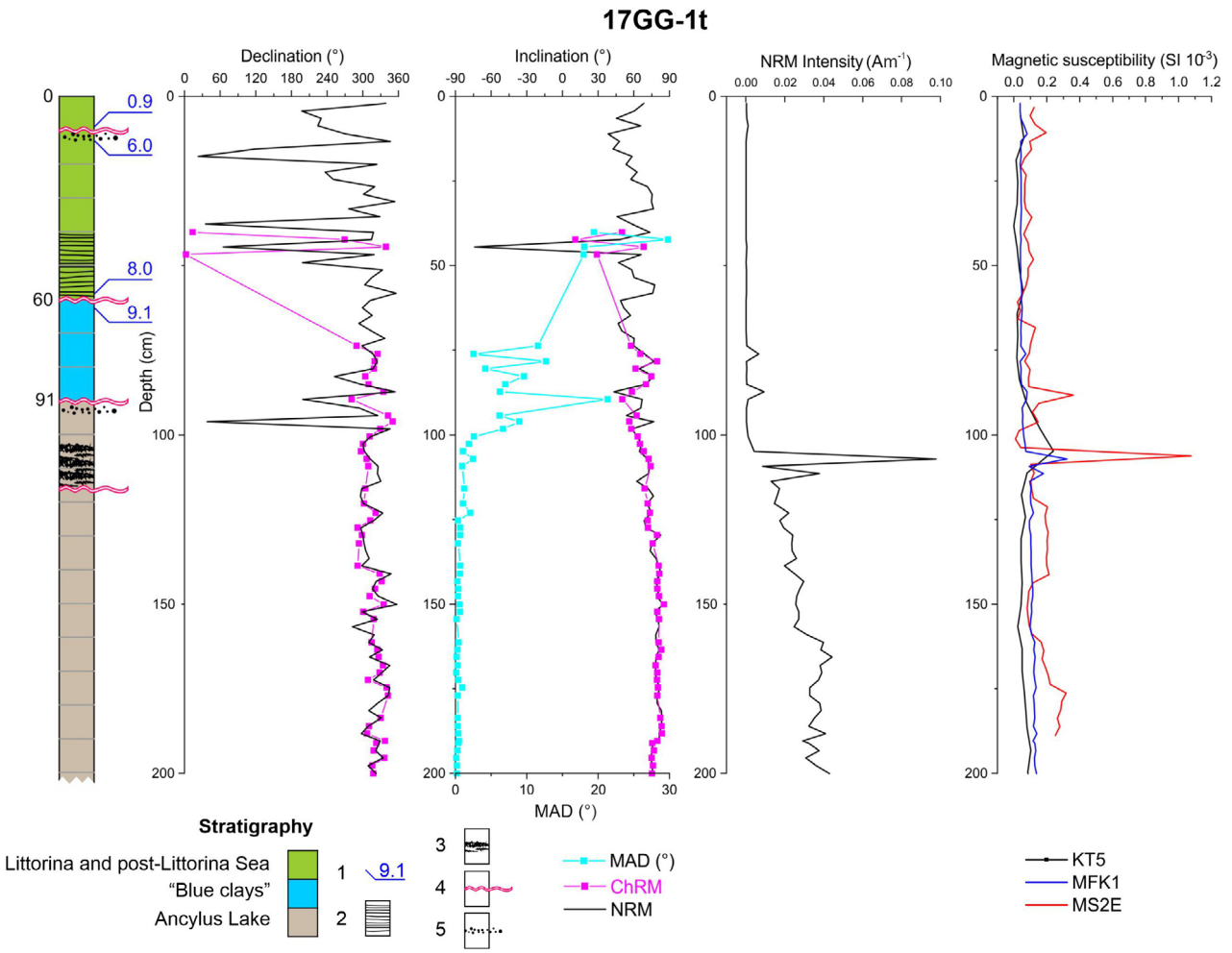

Fig. 11. Palaeomagnetic data and lithology of the 17GG-1t core (upper 200 cm). Declination and inclination of the characteristic remanent magnetization (ChRM) are shown by pink lines; solid pink squares mark the AF demagnetized samples. Black lines indicate the natural remanent magnetization (NRM): declination, inclination and magnetization intensity. Maximum angular deviation (MAD) is shown by a light blue line. Data on magnetic susceptibility are obtained with different kappameters: dark blue is MFK1-AF, red is MS2E and black is KT-5.

Figure 12 presents the results of anisotropy of magnetic susceptibility measurements in 119 samples of the 17GG-1t core (0–260 cm interval) with the respective orientation of the three ellipsoid axes (k_{max}, k_{int} and k_{min}). It should be noted that k_{min} axes have steep inclinations, whereas k_{max} and k_{int} lie in the horizontal plane without any distinguishable pattern.

Discussion

Implications from the high-resolution sedimentology and acoustic data

Interpretation of AUs was based on the results of the previous research data analyses (Spiridonov *et al.* 1988, 2007; Winterhalter 1992; Petrov 2010 and archive data available for reinterpretation). Using this approach, we have interpreted the AUs and attributed them to the main phases in the development of the Baltic Sea post-glacial basins – the Baltic Ice Lake, Ancylus Lake and the Littorina Sea (Spiridonov *et al.* 2007; Ryabchuk *et al.* 2020b; Table 3).

According to the acoustic data and using comparison with geological (core description) data, AU5 has been interpreted as glacial till from the Late Pleistocene, with a highly dissected surface. Within some areas (for example, sedimentary basin 8E), the surface of the Last Glacial till is represented by several large ridges with small subparallel ridges of the De Geer moraine (Ryabchuk *et al.* 2018). Dense and distinctly laminated brownish varved clays of about 5 m thick represent AU4, with an average thickness of about 6 m. The next unit, AU3 (with a maximal thickness of 8–9 m) is represented by less dense thin-laminated (1 mm and less) to homogenous brownish clays of the Baltic Ice Lake sediments (with an average thickness of about 5 m). The AU2 unit has been described as brownish-grey clays with

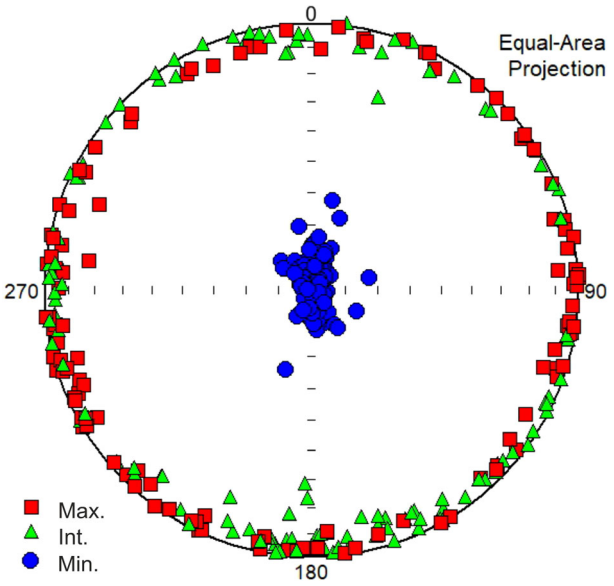

Fig. 12. Results of the anisotropy of magnetic susceptibility measurements performed on 119 samples (0–260 cm) from the 17GG-1t core. Stereographic projections of the directions of the principal susceptibility axes: k_{max} (red squares), k_{int} (green triangles) and k_{min} (blue circles).

black hydrotroillite inclusions and interpreted as the Ancylus Lake sediments. Since they are thin layers (up to 30 cm), 'blue clays' were not identified on SBP profiles. Finally, AU1 consists of soft olive-grey to black sediments that have been interpreted as Littorina Sea deposits. The average thickness of these postglacial deposits is 12–15 m (although this varies from 0 to 30, 0 to 20 and 2 to 23 m within core sampling areas 8W, 8E and 2, respectively; Figs 1, 4, 6, 8, Table 1).

Sedimentary conditions in the EGoF during the postglacial to Holocene period

The Ancylus Lake. – The data obtained allowed regional features to be identified in the development of the palaeobasins 8W, 8E, 3 and 2 (Fig. 1) in the EGoF. A catastrophic palaeoenvironmental event – the Baltic Ice Lake drainage – was shown to have preceded the start of Holocene sedimentation. The water level fell dramatically, and sedimentary conditions were completely altered. The event is clearly reflected in the EGoF for all acoustic profiles with a distinct acoustic boundary marking the stratigraphical unconformity (Figs 4, 6). The boundary was traced in two of the core sections studied, shown by a sharp change in the lithology (in the 17GG-1t and 18MI-1t cores; Figs 5A, 7A), and by an erosion surface (for example, in the 17GG-1t core; Fig. 7A).

Along with 'pre-Ancylus' regression, a grain size coarser than in the Baltic Ice Lake sediments indicates a transgressive–regressive cycle east of Gogland Island (Figs 1, 5). Unfortunately, AMS ^{14}C dating of the described sediment unit (183–184 cm horizon in the 18MI-1t core and 90–92 cm in the 17GG-1t core) did not demonstrate consistent results. The age of the sediments (18.8 and 12.6 ka BP, respectively) contradicts the existing understanding of the Baltic Sea basin development, and that the sediments are in fact likely to be younger than these dates show (Andrén *et al.* 2011). It is well known that dating of glaciolacustrine and glaciofluvial sediments, which typically have low TOC content is always problematic, due to possible redeposition of organic carbon from older strata as a result of the erosion processes (Olsen *et al.* 2001). The low TOC content during the Ancylus Lake stage also indicates low bioproductivity at that time. Vertical grain-size and geochemical parameter distributions demonstrate weak variability throughout the core section, indicating relatively calm deep-water conditions and slow environmental changes. Significant fluctuations in the concentrations of chemical elements (e.g. an increase in S content) are observed only within the 'hydrotroillite horizons'. Keeping in mind the possible presence of hiatuses, the estimated sedimentation rates of the Ancylus Lake unit are more than 1.6 mm a^{-1}. The relatively low Br concentration and calculated palaeosalinity (2–3‰) indicate freshwater conditions prevailed in the lake.

No evidence of saltwater intrusion by the Yoldia Sea into the Baltic Ice Lake was discovered in the bottom of the Gulf of Finland during our investigations.

Pre-Littorina regression (transitional 'blue clays' layer). – According to existing understanding, based mainly on onshore palaeolimnological and geoarchaeological studies (Rosentau *et al.* 2013), the final phase of development of the Ancylus Lake in the EGoF was regressive. The first saline water inflows into the Baltic Sea basin have been linked to the post-Ancylus (pre-Littorina) phase (Grigoriev *et al.* 2011).

The 'blue clays', which usually represent the transitional layer from freshwater to the marine environment in the northern Baltic, the Gulf of Bothnia, and the Gulf of Finland, were recovered in the studied cores from the east of Gogland Island and near Moshchny Island (Fig. 1). The deposits of 'blue clays' are characterized by a sharp peak on the magnetic susceptibility curves. The occurrence of pyrite microconcretions has been confirmed by X-ray diffraction analysis (d (Å): 1.630, 2.689, 1.041). The content of pyrite, which makes up the entire heavy mineral fraction of 'blue clays', can reach 0.1–0.3% (weight %; Virtasalo *et al.* 2010).

In all the cores studied, 'blue clays' are represented by a lithologically specific layer from 3 to 30 cm thick. Sediments are characterized by a sharp upward change in grain-size composition (grain-size mode shifts towards silt fraction) and geochemical parameters. At the lower boundary of the layer, an increase in LOI value,

TOC, S, Mn, Br contents, and calculated palaeosalinity was observed. The sediments of the 'blue clays' layers in the EGoF were dated (17GG-1t and 18MI-1t cores) for the first time, with the age of 9.1 ka BP.

It is important to note that these specific sediments formed during the transition from lacustrine to marine conditions when the environment in the study area was favourable to the development of benthic fauna. The lower contact of these deposits is either underlain by a sand layer or is characterized by a sharp increase in silt fraction content. A significant gap in sedimentation marked by erosional contact at the base of the Littorina sediments was also identified during the study of the 09F40 core (Virtasalo *et al.* 2014).

The data obtained correspond well to the understanding of palaeogeographical development of the Baltic Sea basin. According to Andrén *et al.* (2011), the transitional phase is characterized by the relative water level drop and by the first weak saline water inflows that occurred into the western Baltic and Bornholm Deep (Andrén *et al.* 2000; Berglund *et al.* 2005). This event has been dated to 9.8–8.5 ka BP and referred to the Initial Littorina Sea (Andrén *et al.* 2000), or Mastogloia Sea.

An abrupt change in sedimentary conditions, under the influence of marine transgression starting at a low initial water level, led to the transformation of the lithological and geochemical features of sediments accumulated in different areas of the Baltic Sea. According to Blazhchishin (1998), in the upper part of the Early Holocene lacustrine sediments (regressive phase) from the Arkona Basin (central Baltic), an interlayer enriched by allochthonous organic detritus is sometimes observed.

In the core section from the submarine platform located at a depth of 45 m, south of the Kriegers-Flak Bank (southern Baltic), the maximum of the Ancylus regression is reflected in the peat layer accumulated under subaerial conditions (Blazhchishin 1998). A layer (5–15 cm thick) of grey sand containing detritus and a complex of diatoms from the Mastogloia Sea is usually distinguished at the contact of Ancylus and Littorina deposits in the western Baltic (Blazhchishin 1998). This horizon is overlain by sandy sapropel in the Arkona Basin and by humic silt 10–30 cm thick in the Mecklenburg Bay (southwestern Baltic Sea). Accumulation of these sediments is associated with further regression of the Mastogloia Sea. The sediments correspond to the lower horizon of thinly laminar sapropels in the deep basins of the central Baltic. These sapropels are replaced by peaty layers in shallow areas (Blazhchishin 1998).

In the Gdansk Basin, the initial stage of marine transgression corresponds to a layer of olive-grey silty clays with rare dark-colour lenticular bands of 1–5 mm thickness and with black microinclusions (Grigoriev *et al.* 2011). In the Gotland and Bornholm Deeps, Harff *et al.* (2011) distinguished deposits of the initial phase of Littorina transgression as an independent horizon (B1). The horizon was formed under reducing conditions with a lack of oxygen at the bottom-water interface and is characterized by well-pronounced lamination (banding).

Littorina and post-Littorina Sea. – The upper lithological unit of the geological sequence is interpreted to include Littorina and post-Littorina sediments. The sediments are characterized by the highest variability in physical and chemical parameters, indicating numerous changes in sedimentary conditions. High-resolution sedimentological research of the studied cores has revealed from one to four erosion surfaces separating the sediment units, each with significantly different grain-size composition and geochemistry. Littorina marine deposits differ from the underlying sediments by colour, structure, and grain-size composition. In the all studied cores, the LOI value and TOC content, as well as calculated palaeosalinity, increase. The data obtained correspond well to the data from the other parts of the Baltic Sea basin. According to some investigations, the sudden increase in TOC content is exclusively coupled to changes in primary production or is partly due to better preservation of carbon during anoxic conditions (Sohlenius *et al.* 1996). Another reason for the rapid increase in LOI in the sediments can be an increase in the Secchi depth due to flocculation of clay particles and subsequent rapid sedimentation due to increased primary production (Winterhalter 1992; Andrén *et al.* 2011).

Dating of Littorina deposits in the three EGoF cores has allowed the comparison of results of sedimentological analyses with the data from the other areas of the Baltic Sea. The age of the basal layer of Littorina deposits in the 17GG-1t core (right above the contact with 'blue clays') has been determined as 8.0 ka BP. This indicates that the typical marine sediments started to accumulate within the Gogland sedimentary basin at the same time as in the western, central and the southeastern Baltic. The data obtained are in accordance with other studies that have shown the same age for this time interval – between 8.5 and 8.0 ka BP (Sohlenius *et al.* 1996; Sohlenius & Westman 1998; Andrén *et al.* 2000).

The first phase of the Littorina Sea in the central Baltic has been dated as 8.1–6.0 ka BP (B1 horizon; Harff *et al.* 2011). It has been described as a transitional phase from brackish water to a marine environment, with anoxic conditions dominating at the near-bottom. The latter favour good preservation of thin sediment lamination undisturbed by benthic organism activity. This time interval corresponds to the lower Littorina sediment unit in the 17GG-1t core dated as 8.0–6.0 ka BP. The bottom layer of the described unit (about 30–40 cm thick) is represented by thin-laminated sediments east of Gogland Island and near Moshchny Island (Fig. 1), indicating anoxic bottom conditions. The thickness of the laminated layer suggests that anoxic conditions existed within the study sedimentary basin between the

transgression onset and its maximum, which occurred at approximately 7.3 ka BP and was caused by climate warming (Miettinen *et al.* 2007). Distribution of geochemical parameters throughout this sediment interval indicates suppressed clastic sediment supply (Grigoriev *et al.* 2011). The occurrence of anoxic sedimentary conditions in the deepest EGoF sedimentary basin 8 during the first stage of the Littorina Sea (8.0–7.3 ka BP), similar to the one established earlier for the central Baltic (Harff *et al.* 2011; Warden *et al.* 2017), is an important finding of the present study. This change in the environment caused by a sea-level rise can be correlated with the atmospheric warming phase, which followed the significant cooling phase 8.8–8.2 ka ago (Sarnthein *et al.* 2003). The occurrence of the cold phase of the Littorina Sea transgression was caused by the melting of the ice sheets in North America; its influence on oceanic circulation resulted in large volumes of cold water entering the North Atlantic Ocean (Von Storch *et al.* 2015). However, our data, as well as other publications concerning the onset of the Littorina transgression (Harff *et al.* 2011; Hyttinen *et al.* in press), do not support the hypothesis that the cold phase lasted several centuries after 8.2 ka BP. Thus, by 8.0 ka BP, the impact of saline waters can be traced throughout the Baltic Sea from Kattegat (Hyttinen *et al.* in press), to the Great Belt (Bennike *et al.* 2004), and to the EGoF.

Deposits accumulated during 7.0–6.0 ka BP are characterized by relatively light colour, absence of lamination, and traces of bioturbation. Similar features have been recognized for the same age intervals in sediment cores from the central Baltic (Warden *et al.* 2017). The sediments sections were formed during the cooling in the Baltic Sea region preceding a dramatic warming phase, which started at approximately 6.0 ka BP. According to an earlier study (Harff *et al.* 2011), the age of this climate change has been estimated as 5.7 ka BP. With commencement of a new period of climate warming, oxic conditions in the bottom-water layer of the central Baltic were followed by anoxic conditions, causing the deposition of a clearly laminated sediment unit.

Low NRM intensity is typical for the Littorina Sea sediments and indicates the low reliability of the estimated ChRM reflected in the high MAD values. However, it is well known that from 7.5–4.5 ka BP, northern Europe and the Barents Sea experienced a significant instability in the geomagnetic field referred to as the Solovki excursion (Gooskova *et al.* 2004; Pospelova 2004). Steep k_{min} inclinations are evident in the 17GG-1t core; at the same time there is no distinguishable pattern in the k_{max} and k_{int} lying in the horizontal plane. This may indicate that sedimentation was occurring under calm water conditions without strong currents (Nowaczyk *et al.* 2001; Tauxe 2010). At the same time, it should be noted that non-sedimentation (or even erosion events) do not affect the structure of already deposited sediments.

The declination and inclination variations within the 10–60 cm level are comparable with the geomagnetic variations expected for 8.0–6.0 ka BP. One of the most comprehensive studies of palaeosecular variations during the Late Pleistocene to Holocene was conducted on lake sediments collected in Great Britain (Creer 1985). According to these data, from 7.5–6.2 ka BP the inclination changed from maximum to minimum, while the declination changed from maximum to minimum, indicating there was a transition. Moreover, in both cases, variations equalled 20°. Despite large scattering in NRM directions in 17GG-1t, a similar variability can be observed (Fig. 11).

Deposits from the initial phase of the Littorina transgression were not preserved near Moshchny Island (Figs 1, 2, 7A, B). In the 18MI-1t core, the upper contact of 'blue clays' is overlain by a sand layer. The bottom layer of the Littorina Sea sediments is dated as 7.1 ka BP. Three interlayers enriched by a sand fraction are distinguished within the layer. The grain-size distribution in the sediments indicates high near-bottom hydrodynamic activity, and variations in sedimentation rates associated with possible erosion events. At the same time, in the 18MI-2t core located at the same part of the sedimentary basin, the lower interval of the Littorina stratigraphical unit (19–41 cm) is characterized by pronounced lamination without any sign of bioturbation. Lithological and geochemical parameters of the deposits are similar to those described in the 17GG-1t core. The latter accumulated under anoxic conditions at the beginning of the Littorina transgression. A decreasing trend in Ti and K concentrations, as well as in ratios of chemical elements indicates the deepening of the basin. An increase in S content is an indicator of an anoxic environment, while an increase in Br content and calculated palaeosalinity indicate marine conditions.

Upcore, laminated sediments are replaced by light bioturbated silty clays (47–67 and 77–87 cm in 18MI-1t and 18MI-2t cores); these accumulated after 6.7 ka BP during an interval of cooling (Warden *et al.* 2017). Data from (Häusler *et al.* 2017) have shown that in the central and northern Baltic, deposition of laminated sediments occurred under water column stratification and hypoxic/anoxic bottom-water conditions. This environment was caused by elevated organic matter levels. In turn, increased primary production is explained by P regeneration from anoxic sediments during the initiation of the Holocene thermal maximum at *c.* 7.0 cal. ka BP. In 18MI-1t, the onset of accumulation after an erosion event is dated to 5.4 ka BP. The occurrence of anoxic conditions coincides again with a period of warming. Similar environmental conditions were prevailing in the central Baltic between 6.0 and 4.8 ka BP (Thermal Optimum; Warden *et al.* 2017).

It is noteworthy that the same age (5.7 ka BP) for laminated Littorina sediments was determined in the

09F40 sediment core located in the central part of sedimentary basin 3 (Fig. 1), to the south of the Berezovye Islands (east of the 18MI-1t and 18-MI-2t core sites) (Virtasalo *et al.* 2014). In the 09F40 core, this stratigraphical unit overlays the Ancylus Lake deposits. The units are separated by an erosion surface enriched with sand. The older Littorina sediments are also absent in the core, indicating the described hiatus during the initial phase of the Littorina transgression was even longer in the central part of this sedimentary basin. High-resolution sedimentological study of the 09F40 core allowed tracing of the continuous sedimentation that has occurred during the last 5.9 ka BP with a dramatic change in sedimentary conditions at about 3.3 ka BP (that is, an erosion surface). The study of the 09F40 core also showed the relationship between sedimentation and climate change (e.g. Holocene Climatic Optimum, Medieval Warm Period and Little Ice Age; Virtasalo *et al.* 2014).

The data obtained north of Shepelevo Cape (17KRG-1 and 17KRG-3 cores) demonstrate that the silty clays accumulated in the easternmost part of the EGoF during the last 3.6 ka BP. An abrupt transition from coarse to fine sediments occurred at about 1.5 ka BP (Fig. 9). The same trend in grain size was observed in the 09F40 core (Virtasalo *et al.* 2014). The grain-size composition of the deposits from the western part of sedimentary basin 2 indicates their accumulation in the shallow environment from 3.5–1.8 ka BP. The overlying younger sediments (from the last 2 ka) accumulated in a deeper sea. The results support the hypotheses proposing a sea-level drop of a relatively small amplitude in the easternmost part of the EGoF at about 3.5 ka BP followed by transgression revealed through on-land research results (Ryabchuk *et al*. 2016).

Conclusions

A specific transitional layer of 'blue clays' formed during the Ancylus Lake regression indicates the first stage of brackish water inflow into the Gulf of Finland under oxygen-rich conditions. The age of the 'blue clays' is *c*. 9.1 ka BP.

Littorina marine sedimentation in the western part of the study area began after 8.0 ka BP (the first stage corresponding with a warming period from 8.0–7.0 ka BP) under conditions of oxygen deficiency. From 7.0–6.0 ka BP, sedimentary conditions in the EGoF were characterized by the predominance of oxygen-rich conditions and active processes of bioturbation. Specific relationships as 'warming – transgression – anoxic conditions' and 'cooling – regression – oxygen-rich conditions' have been revealed. Holocene cycles of hypoxia associated with periods of warming have further been identified.

During the 6.0–4.8 ka BP period (Holocene Climatic Optimum), the accumulation of undisturbed silty clays with subhorizontal lamination occurred under anoxic conditions. The interval from 4.8–2.0 ka BP was dominated by oxygen-rich near-bottom conditions favourable for benthic organisms.

The grain-size distributions throughout the sediment cores taken east of the Berezovye Islands suggest that there was a relative lowering in sea level from 3.5–1.8 ka BP, followed by a rise. The data obtained in the present study confirm earlier conclusions about sea-level fluctuations based on analysis of the distribution and structure of coastal accumulative forms and submarine platforms (Amantov *et al*. 2012, 2013; Ryabchuk *et al*. 2016).

Several erosion surfaces were described in the studied sediment cores. Initiation of the Littorina silty clay sedimentation appeared at different times: after 8.0 ka BP near Gogland Island; after 7.0 ka BP near Moshchny Island; and after 5.9 ka BP near the Berezovye Islands. In the vicinity of Gogland and Moshchny Islands, the commencement (after a long hiatus) of the accumulation of a new cycle of silty clays from 0.95–0.7 ka BP corresponds to the Medieval Climatic Optimum.

A significant change in magnetic and palaeomagnetic properties of the sediments marks the transition from the Ancylus Lake to the Littorina Sea. While the Ancylus sediments have higher magnetic susceptibility, the Littorina Sea unit is characterized by fluctuations in ChRM and NRM directions. The latter is typical for northern Europe deposits of 7.5–4.5 ka BP age. Moreover, palaeosecular variations observed in the 17GG-1t core coincide with the data obtained for northern Europe.

Acknowledgements. – Acoustic data analyses and interpretation was carried out under project No. 17-7720041 of Russian Science Foundation. Palaeomagnetic study, multibeam data analyses and interpretation were undertaken with support of the Russian Foundation for Basic Research grant No. 19-05-00768. Interpretation of LOI and TOC analysis was partly supported by the state assignment of IO RAS (Theme No. 0149-2019-0013). We acknowledge two anonymous reviewers for valuable comments that greatly improved this manuscript. Prof. Cherith Moses is warmly thanked for the English editing.

Author contributions. – DR: methodology (lead), supervision (lead), writing – original draft (lead); AS: investigation (lead), software (lead), visualization (lead), writing – original draft (lead); DP: investigation (lead), writing – original draft (lead); VZ: investigation (lead), supervision (lead), writing – original draft (lead); DE: investigation (equal), writing – original draft (equal); AP: investigation (equal), writing – original draft (equal); LDB: investigation (equal), writing – original draft (equal); EP: investigation (equal), writing – original draft (equal); LMB: investigation (equal), software (equal), visualization (equal); AG: investigation (lead); AE: investigation (equal).

References

Amantov, A., Ryabchuk, D., Fjeldskaar, W., Zhamoida, V. & Amantova, M. 2013: Possible role of hydroisostasy in peculiarities of lateglacial-postglacial sedimentation of the eastern part of the Gulf of Finland and Lake Ladoga. *EGU General Assembly Conference Abstracts 15*, EGU2013-8561.

Amantov, A. V., Zhamoida, V. A., Ryabchuk, D. V., Spiridonov, M. A. & Sapelko, T. V. 2012: Geological structure of submarine terraces of the eastern Gulf of Finland and modeling of their development

during postglacial time. *Regional Geology and Metallogeny 50*, 5–27 (in Russian).

Andrén, E., Andrén, T. & Sohlenius, G. 2000: The Holocene history of the southwestern Baltic Sea as reflected in a sediment core from the Bornholm Basin. *Boreas 29*, 233–250.

Andrén, T., Björck, S., Andrén, E., Conley, L. Z. & Anjar, J. 2011: The development of the Baltic Sea Basin during the last 130 ka. *In* Harff, J., Björck, S. & Hoth, P. (eds.): *The Baltic Sea Basin*, 75–97. Springer, Berlin-Heidelberg.

Bennike, O., Jensen, J. B., Lemke, W., Kuijpers, A. & Lomholt, S. 2004: Late- and postglacial history of the Great Belt, Denmark. *Boreas 33*, 18–33.

Berglund, B. E., Sandgren, P., Barnekow, L., Hannon, G., Jiang, H., Skog, G. & Yu, S. Y. 2005: Early Holocene history of the Baltic Sea, as reflected in coastal sediments in Blekinge, southeastern Sweden. *Quaternary International 130*, 111–139.

Blazhchishin, A. I. 1998: *Palaeogeography and Evolution of Late Quaternary Sedimentation in the Baltic Sea*. 160 pp. Yantarny Skaz, Kaliningrad (in Russian).

Budanov, L. M., Sergeev, A Yu, Ryabchuk, D. V., Zhamoida, V. A. & Khorikov, V. I. 2019: Geoenvironmental zoning of the eastern Gulf of Finland bottom. *Regional Geology and Metallogeny 79*, 23–34 (in Russian).

Creer, K. M. 1985: Review of lake sediment palaeomagnetic data. *Geophysical Surveys 7*, 125–160.

Dudzisz, K., Szaniawski, R., Michalski, K. & Manby, G. 2016: Applying the anisotropy of magnetic susceptibility technique to the study of the tectonic evolution of the West Spitsbergen Fold-and-Thrust Belt. *Polar Research 35*, 31683, https://doi.org/10.3402/polar.v35.31683.

Gooskova, E. G., Raspopov, O. M., Piskarev, A. L., Dergachev, V. A. & Mörner, N. A. 2004: Geomagnetic field fine structure for the last 30 kyr based on the magnetization of the Barents sea sediments. *Geomagnetism and Aeronomy 44*, 510–516.

Gordeeva, S. M. & Malinin, V. N. 2014: *Gulf of Finland Sea Level Variability*. 179 pp. RSHU Publishers, St. Petersburg (in Russian).

Grigoriev, A., Zhamoida, V., Spiridonov, M., Sharapova, A., Sivkov, V. & Ryabchuk, D. 2011: Late-glacial and Holocene palaeoenvironments in the Baltic Sea based on a sedimentary record from the Gdansk Basin. *Climate Research 48*, 13–21.

Gudelis, V. K. & Emelyanov, E. M. (eds.) 1976: *Geology of the Baltic Sea*. 383 pp. Moxlas, Vilnius (in Russian).

Harff, J., Endler, R., Emelyanov, E., Kotov, S., Leipe, T., Moros, M., Olea, R., Tomczak, M. & Witkowski, A. 2011: Late Quaternary climate variations reflected in Baltic Sea sediments. *In* Harff, J., Björck, S. & Hoth, P. (eds.): *The Baltic Sea Basin*, 99–132. Springer, Berlin, Heidelberg.

Harff, J., Deng, J., et al. 2017: What Determines the Change of Coastlines in the Baltic Sea?. *In* Harff, J., Furmanczyk, K. & Von Storch, S. (eds.): *Coastline Changes of the Baltic Sea from South to East*, 15–35. Springer, Berlin, Heidelberg.

Häusler, K., Moros, M., Wacker, L., Hammerschmidt, L., Dellwig, O., Leipe, T., Kotilainen, A. & Arz, H. W. 2017: Mid- to late Holocene environmental separation of the northern and central Baltic Sea basins in response to differential land uplift. *Boreas 46*, 111–128.

Hyttinen, O., Quintana Krupinski, N., Bennike, O., Wacker, L., Filipsson, H., Obrochta, S., Jensen, J. B., Lougheed, B., Ryabchuk, D., Passchier, S., Snowball, I., Herrero-Bervera, E., Andrén, T. & Kotilainen, A. T. 2020: Deglaciation dynamics of the Fennoscandian Ice Sheet in the Kattegat, the gateway between the North Sea and the Baltic Sea Basin. *Boreas*, https://doi.org/10.1111/bor.12494. ISSN 0300-9483.

Ignatius, H. 1958: On the rate of sedimentation in the Baltic Sea. *Bulletin of the Geological Society of Finland 180*, 135–145.

Ignatius, H., Kukkonen, E. & Winterhalter, B. 1968: Notes on a pyritic zone in upper Ancylus sediments from the Bothnian Sea. *Bulletin of the Geological Society of Finland 40*, 131–134.

Jensen, J. B., Moros, M., Endler, R., & IODP Expedition 347 Members 2017: The Bornholm Basin, southern Scandinavia: a complex history from Late Cretaceous structural developments to recent sedimentation. *Boreas 46*, 3–17.

Kaskela, A. M., Rousi, H., Ronkainen, M., Orlova, M., Babin, A., Gogoberidze, G., Kostamo, K., Kotilainen, A. T., Neevin, I., Ryabchuk, D., Zhamoida, V. & Sergeev, A. 2017: Linkages between benthic assemblages and physical environmental factors: The role of geodiversity in Eastern Gulf of Finland ecosystems. *Continental Shelf Research 142*, 1–13.

Kirschvink, J. L. 1980: The least-squares line and plane and the analysis of palaeomagnetic data. *Geophysical Journal International 62*, 699–718.

Kotilainen, A. T., Arppe, L., Dobosz, S., Jansen, E., Kabel, K., Karhu, J., Kotilainen, M. M., Kuijpers, A., Lougheed, B. C., Meier, H. M., Moros, M., Neumann, T., Porsche, C., Poulsen, N., Rasmussen, P., Ribeiro, S., Risebrobakken, B., Ryabchuk, D., Schimanke, S., Snowball, I., Spiridonov, M., Virtasalo, J., Weckstrom, K., Witkowski, A. & Zhamoida, V. 2014: Echoes from the past: a healthy Baltic Sea requires more effort. *Ambio 43*, 60–68.

Leipe, T., Tauber, F., Vallius, H., Virtasalo, J., Uścinowicz, S., Kowalski, N., Hille, S., Lindgren, S. & Myllyvirta, T. 2011: Particulate organic carbon (POC) in surface sediments of the Baltic Sea. *Geo-Marine Letters 31*, 175–188.

Lyahin, Y. I. 1994: *Recent Ecological Conditions of CIS Seas*. 55 pp. RGGMI, St. Petersburg (in Russian).

Mattila, J., Kankaanpaa, H. & Ilus, E. 2006: Estimation of recent sediment accumulation rates in the Baltic Sea using artificial radionuclides $_{137}$Cs and $_{239,240}$Pu as time markers. *Boreal Environment Research 11*, 95–107.

Miettinen, A., Savelieva, L., Subetto, D. A., Dzhinoridze, R., Arslanov, K. & Hyvärinen, H. 2007: Palaeoenvironment of the Karelian Isthmus, the easternmost part of the Gulf of Finland, during the Litorina Sea stage of the Baltic Sea history. *Boreas 36*, 441–458.

Nezhikhovsky, R. A. 1988: *Problems of Neva River and the Neva Bay Hydrology*. 103 pp. Hydrometeoizdat, Leningrad (in Russian).

Nowaczyk, N. R. 2003: Detailed study on the anisotropy of magnetic susceptibility of arctic marine sediments. *Geophysical Journal International 152*, 302–317.

Nowaczyk, N. R., Antonow, M., Knies, J. & Spielhagen, R. F. 2003: Further rock magnetic and chronostratigraphic results on reversal excursions during the last 50 ka as derived from northern high latitudes and discrepancies in precise AMS ^{14}C dating. *Geophysical Journal International 155*, 1065–1080.

Nowaczyk, N. R., Frederichs, T. W., Kassens, H., Nørgaard-Pedersen, N., Spielhagen, R. F., Stein, R. & Weiel, D. 2001: Sedimentation rates in the Makarov Basin, central Arctic Ocean: a paleomagnetic and rock magnetic approach. *Paleoceanography 16*, 368–389.

Olsen, L., Van der Borg, K., Bergstrøm, B., Sveian, H., Lauritzen, S.-E. & Hansen, G. 2001: AMS radiocarbon dating of glacigenic sediments with low organic carbon content- an important tool for reconstructing the history of glacial variations in Norway. *Norwegian Journal of Geology 81*, 59–92.

Petrov, O. V. 2010: *Atlas of Geological and Environmental Geological Maps of the Russian Area of the Baltic Sea*. 78 pp. VSEGEI, Saint-Petersburg.

Pospelova, G. A. 2004: Geomagnetic excursions. *In* Burlatskaya, S. P., Didenko, A. N. & Sharonova, Z. V. (eds.): *Brief History and Modern State of Geomagnetic Research at the Institute of Physics of the Earth RAS: Collected Papers*, 44–55, IPE RAS, Moscow (in Russian).

Rasmus, K., Kiirikki, M. & Lindfors, A. 2015: Long-term field measurements of turbidity and current speed in the Gulf of Finland leading to an estimate of natural resuspension of bottom sediment. *Boreal Environment Research 20*, 735–747.

Raukas, A. 1994: Yoldia stage – the least clear interval in the Baltic Sea history. *Baltica 8*, 5–14.

Reimer, P. J., Bard, E., Bayliss, A., Beck, J. W., Blackwell, P. G., Ramsey, C. B., Buck, C. E., Cheng, H., Edwards, R. L., Friedrich, M., Grootes, P. M., Guilderson, T. P., Haflidason, H., Hajdas, I., Hatté, C., Heaton, T. J., Hogg, A. G., Hughen, K. A., Kaiser, K. F., Kromer, B., Manning, S. W., Niu, M., Reimer, R. W., Richards, D. A., Scott, E. M., Southon, J. R., Turney, C. S. M. & van der Plicht, J. 2013: IntCal13 and Marine13 radiocarbon age calibration curves 0–50,000 years cal BP. *Radiocarbon 55*, 1869–1887.

Renberg, I., Bränvall, M. L., Bindler, R. & Emteryd, O. 2002: Stable lead isotopes and lake sediments – a useful combination for the study of

atmospheric lead pollution history. *The Science of the Total Environment 292*, 45–54.
Rosentau, A., Muru, M., Kriiska, A., Subetto, D. A., Vassiljev, J., Hang, T., Gerasimov, D., Nordqvist, K., Ludikova, A., Lõugas, L. & Raig, H. 2013: Stone Age settlement and Holocene shore displacement in the Narva-Luga Klint Bay area, eastern Gulf of Finland. *Boreas 42*, 912–931.
Ryabchuk, D., Kolesov, A., Chubarenko, B., Spiridonov, M., Kurennoy, D. & Soomere, T. 2011: Coastal erosion processes in the eastern Gulf of Finland and their links with geological and hydrometeorological factors. *Boreal Environment Research 16* (Suppl. A), 117–137.
Ryabchuk, D., Zhamoida, V., Amantov, A., Sergeev, A., Gusentsova, T., Sorokin, P., Kulkova, M. & Gerasimov, D. 2016: Development of the coastal systems of the easternmost Gulf of Finland, and their links with Neolithic-Bronze and Iron Age settlements. *In* Harff, J., Bailey, G. & Luth, F. (eds.): *Geology and Archaeology: Submerged Landscapes of the Continental Shelf*, 51–76. *Geological Society, London, Special Publications 411*.
Ryabchuk, D. V., Grigoryev, A. G., Sapelko, T. V., Zhamoida, V. A., Kotilayiei, A. T., Sergeev, A. Yu. & Budanov, L. M. 2017: Sedimentation processes of the postglacial basins based on study of bottom sediments of the Eastern Gulf of Finland. *Bulletin of the Russian Geographical Society 149*, 32–52 (in Russian).
Ryabchuk, D., Sergeev, A., Krek, A., Kapustina, M., Tkacheva, E., Zhamoida, V., Budanov, L., Moskovtsev, A. & Danchenkov, A. 2018: Geomorphology and Late Pleistocene-Holocene sedimentary processes of the Eastern Gulf of Finland. *Geosciences 8*, 102, doi: 10.3390/geosciences8030102
Ryabchuk, D., Orlova, M., Kaskela, A., Kotilainen, A., Sergeev, A., Sukhacheva, L., Zhamoida, V., Budanov, L. & Neevin, I. 2020a: The eastern Gulf of Finland—brackish water estuary under natural conditions and anthropogenic stress. *In* Harris, T. & Baker, K. (eds.): *Seafloor Geomorphology as Benthic Habitat*, 281–301, Elsevier, London.
Ryabchuk, D., Sergeev, A., Zhamoida, V., Budanov, L., Krek, A., Neevin, I., Bubnova, E., Danchenkov, A. & Kovaleva, O. 2020b: High-resolution geological mapping towards an understanding of post-glacial development and Holocene sedimentation processes in the eastern Gulf of Finland: an EMODnet Geology case study. *In* Asch, K., Kitazato, H. & Vallius, H. (eds.): *From Continental Shelf to Slope: Mapping the Oceanic Realm. Geological Society, London, Special Publications 505*.
Sagnotti, L. 2013: Demagnetization Analysis in Excel (DAIE). An open source workbook in Excel for viewing and analyzing demagnetization data from paleomagnetic discrete samples and u-channels. *Annals of Geophysics 56*, D0114, https://doi.org/10.4401/ag-6282.
Sandgren, P., Subetto, D. A., Berglund, B. E., Davydova, N. N. & Savelieva, L. A. 2004: Mid-Holocene Littorina Sea transgressions based on stratigraphic studies in coastal lakes of NW Russia. *GFF 126*, 363–380.
Sarnthein, M., van Kreveld, S., Erlenkeuser, H., Grootes, P. M., Kucera, M., Pflaumann, U. & Schulz, M. 2003: Centennial-to-millennial-scale periodicities of Holocene climate and sediment injections off the western Barents shelf, 75°N. *Boreas 32*, 447–461.
Shishkina, O. V., Pavlova, G. A. & Bykova, V. S. 1969: *Geochemistry of Halogens in the Marine and Oceanic Sediments and Pore Waters*. 118 pp. Nauka, Moscow (in Russian).
Snezhinsky, V. A. 1951: *Practical Oceanography*. 559 pp. GIMIZ, Leningrad (in Russian).
Sohlenius, G. & Westman, P. 1998: Salinity and redox alternations in the northwestern Baltic proper during the late Holocene. *Boreas 27*, 101–114.
Sohlenius, G., Sternbeck, J., Andrén, E. & Westman, P. 1996: Holocene history of the Baltic Sea as recorded in a sediment core from the Gotland Deep. *Marine Geology 134*, 183–201.
Sokolov, A. N. 2016: *Hydrological Regime of Neva River on the Segment of Major Waterworks Nowadays*. 65 pp. RSHU Publishers, St. Petersburg (in Russian).
Spiridonov, M. A., Rybalko, A. E., Butylin, V. P., Spiridonova, E. A., Zhamoida, V. A. & Moskalenko, P. E. 1988: Modern data, facts and views on the geological evolution of the Gulf of Finland. *Geological Survey of Finland Special Paper 6*, 95–100.
Spiridonov, M., Ryabchuk, D., Kotilainen, A., Vallius, H., Nesterova, E. & Zhamoida, V. 2007: The Quaternary deposits of the eastern Gulf of Finland. *Geological Survey of Finland Special Paper 45*, 5–17.
Tauxe, L. 2010: *Essentials of Paleomagnetism*. 489 pp. University of California Press, Berkeley.
Virtasalo, J. J., Bonsdorff, E., Moros, M., Kabel, K., Kotilainen, A. T., Ryabchuk, D., Kallonen, A. & Hämäläinen, K. 2011: Ichnological trends along an open-water transect across a large marginal-marine epicontinental basin, the modern Baltic Sea. *Sedimentary Geology 241*, 40–51.
Virtasalo, J. J., Löwemark, L., Papunen, H., Kotilainen, A. T. & Whitehouse, M. J. 2010: Pyritic and baritic burrows and microbial filaments in postglacial lacustrine clays in the northern Baltic Sea. *Journal of the Geological Society 167*, 1185–1198.
Virtasalo, J. J., Ryabchuk, D., Kotilainen, A. T., Zhamoida, V., Grigoriev, A., Sivkov, V. & Dorokhova, E. 2014: Middle Holocene to present sedimentary environment in the easternmost Gulf of Finland (Baltic Sea) and the birth of the Neva River. *Marine Geology 350*, 84–96, https://doi.org/10.1016/j.margeo.2014.02.003.
Von Storch, H., Omstedt, A., Pawlak, J., Reckermann, M., Borzenkova, I., Zorita, E. & Koff, T. 2015: *Second Assessment of Climate Change for the Baltic Sea Basin*. 501 pp. Springer, London.
Warden, L., Moros, M., Neumann, T., Shennan, S., Timpson, A., Manning, K., Sollai, M., Wacker, L., Perner, K., Häusler, K., Leipe, T., Zillén, L., Kotilainen, A., Jansen, E., Schneider, R. R., Oeberst, R., Arz, H. & Sinninghe Damsté, J. S. 2017: Climate induced human demographic and cultural change in northern Europe during the mid-Holocene. *Scientific Reports 7*, 15251, https://doi.org/10.1038/s41598-017-14353-5.
Winterhalter, B. 1992: Late-Quaternary stratigraphy of Baltic Sea basins—a review. *Bulletin of the Geological Society of Finland 64*, 189–194.
Zillén, L., Lenz, C. & Jilbert, T. 2012: Stable lead (Pb) isotopes and concentrations – a useful independent dating tool for Baltic Sea sediments. *Quaternary Geochronology 8*, 41–45.

Supporting Information

Additional Supporting Information may be found in the online version of this article at http://www.boreas.dk.

Fig. S1. Geochemical parameters of the 17GG-1t, 18GG-1t and 18GG-2t cores.

Fig. S2. Photographs, grain-size distributions and geochemical parameters of the 17SOM-1 and 17SOM-2 cores.

Fig. S3. Geochemical parameters of the 18MI-1t and 18MI-2t cores.

Fig. S4. Geochemical parameters of the 17KRG-1 and 17KRG-3 cores.